

# Influence of welding parameters on weld quality and productivity using metal cored wires

by

KIMON DROSOS, STAVROS KOTSAKIS

**Diploma work No. 133/2014**

at Department of Materials and Manufacturing Technology  
CHALMERS UNIVERSITY OF TECHNOLOGY  
Gothenburg, Sweden

Diploma work in the Master programme Materials Engineering, Quality and Operations Management

**Performed at:** Chalmers University of Technology  
Department of Materials and Manufacturing Technology  
SE – 412 96 Gothenburg Sweden

**Supervisor(s):** Prof. Peter Hammersberg  
Department of Materials and Manufacturing Engineering  
Chalmers University of Technology, SE- 412 96 Gothenburg

Prof. Lars-Erik Svensson  
Department of Production Technology  
University West, SE – 461 86 Trollhättan

**Examiner:** Prof. Peter Hammersberg  
Department of Materials and Manufacturing Engineering  
Chalmers University of Technology, SE- 412 96 Gothenburg

Influence of welding parameters on weld quality and productivity using metal cored wires  
KIMON DROSOS, STAVROS KOTSAKIS

© KIMON DROSOS, STAVROS KOTSAKIS, 2014

Diploma work no [133/2014](#)  
Department of Materials and Manufacturing Technology  
Chalmers University of Technology  
SE-412 96 Gothenburg  
Sweden  
Telephone + 46 (0)31-772 1000

[[printing office name](#)]  
Gothenburg, Sweden [2014](#)

## Abstract

Robotic Gas Metal Arc Welding (GMAW) is used in fatigue loaded structures where demands on weld quality are very high. Bead dimensions of a weld such as penetration bead thickness and toe radius can reveal whether a weld can reach high fatigue life. However, several welding parameters have high impact on these dimensions. From previous research it has been indicated that geometrical parameters such as torch angle, weld position, push or pull direction etc. are the most influential ones concerning quality of a weld with solid wires. Welding technology offers solid or metal cored wires for robotic GMAW. Even though metal cored wires depict several advantages compared to solid, a lot of skepticism is faced among industries due to its higher cost. Response parameters of a fillet weld by robotized GMAW using metal cored wire were investigated as a function of welding geometry parameters. The goal is to reveal the optimal settings aiming at as high productivity as possible.

Iteration of welding tests using solid wire has been made in order to depict repeatability of previous test results with the same settings. Next step consisted of several series of experiments varying geometrical parameters using metal cored electrode. Repetition of this series for different values of wire feed rate has been carried out and comparisons are made. In order to reveal higher possible productivity, a few tests were carried out for the optimal welds from previous steps for different welding speeds and with pulsed welding. Specimens were cut, grinded and etched. Measurement of weld dimensions was performed via Lumenera software. Analysis of the results was made with JMP 11 software by SAS.

Results indicated that for metal cored wire the majority of high quality welds were performed in push direction, PA position and gun angle of 35°. Correlation analysis showed the nature of the relationships between input and output parameters. Prediction models were constructed for all weld dimensions using regression analysis. Tests with higher welding speeds suggest that there are possibilities for productivity improvement. Pulsed welding revealed that only a trade-off between values of bead thickness and penetration can create a quality weld. Less total amount of high quality welds are observed in pulsed welding, in comparison with conventional welding.

Keywords: fatigue loaded structures, GMAW, solid wire, metal cored wire, weld quality, bead geometry, welding geometry parameters, regression analysis, optimization, modeling, pulsed welding.

## Abbreviations and Symbols

GMAW	Gas Metal Arc Welding
MIG	Metal Inert Gas
MAG	Metal Active Gas
VCE	Volvo Construction Equipment
if	Penetration in the flange plate
iw	Penetration in the waist plate
Lf	Leg length in the flange plate
Lw	Leg length in the waist plate
tf	Toe radius in the flange plate
tw	Toe radius in the waist plate
a	Bead thickness
WF	Wire feed rate
MC	Metal Cored
GMAW-P	Gas Metal Arc Welding-Pulsed

## Table of Contents

<b>Abstract .....</b>	<b>3</b>
<b>Abbreviations and Symbols.....</b>	<b>4</b>
<b>1. Introduction.....</b>	<b>7</b>
1.1 Background .....	7
1.2 Purpose .....	7
1.3 Problem analysis .....	7
1.4 Delimitations.....	8
<b>2. Theory.....</b>	<b>11</b>
2.1 GMAW .....	11
2.1.1 GMAW parameters .....	12
2.1.1.1 Productivity parameters.....	12
2.1.1.2 Geometrical parameters .....	13
2.1.2 GMAW Consumables.....	13
2.1.2.1 Solid electrode.....	13
2.1.2.2 Cored wire.....	14
2.1.3 Welding Technology .....	16
2.1.3.1 Metal Transfer .....	16
2.1.3.2 Pulsed Technology .....	17
2.2 Statistical analysis.....	18
2.2.1 Linear regression .....	18
2.2.2 Scatter plot and correlation analysis .....	19
<b>3. Experimental Process.....</b>	<b>21</b>
3.1 Welding process.....	21
3.1.1 Welding Parameters .....	21
3.1.2 Base Material .....	23
3.1.3 Robotic welding.....	23
3.1.4 Electrodes.....	25
3.2 Sample preparation.....	26
3.3 Measurement .....	28
3.4 Statistical Analysis .....	30
<b>4. Results .....</b>	<b>31</b>
4.1 Step A .....	31
4.2 Step B & C.....	32
4.2.1 Mean values and standard deviations .....	32
4.2.2 Distributions .....	33
4.2.3 Bivariate relationships.....	34
4.2.4 Prediction models.....	39
4.3 Step D .....	42
4.4 Step E – Pulsed welding.....	44
<b>5. Discussion .....</b>	<b>49</b>
<b>6. Conclusions.....</b>	<b>53</b>
References.....	55
Appendix A – Experiments.....	57



# 1. Introduction

## 1.1 Background

Tee-joint, which is a specific type of fillet weld where two perpendicular metal plates are welded together, has a broad application in industry. The most important welding dimensions, which indicate the quality of a Tee-joint, are bead thickness, penetration and toe radius of the weld (Hammersberg, & Olsson 2013).

In Gas Metal Arc Welding (GMAW) a set of different process parameters determine the final weld dimensions and geometry. Examples of such parameters are voltage, current, wire feed speed, travelling speed or gun angle (Hammersberg, & Olsson 2013).

In a previous research carried out by Chalmers University of Technology and Volvo Construction Equipment (VCE), weld dimensions were investigated as a function of welding geometrical control parameters in robotised MAG welding. Gun angle, slit between the plates, welding position, slope and push/pull factor were the control parameters, which were in focus in this study. The results of the analysis indicated that when determining the welding geometry, the influence of geometrical parameters such as torch angle and plate position was of primary importance rather than productivity parameters such as voltage, current and welding speed. (Hammersberg & Olsson 2013).

## 1.2 Purpose

The purpose of this thesis project is to test metal cored wires by investigating the influence of different GMAW welding process parameters on the final weld geometry, and especially on penetration, toe radius and bead thickness. This will be achieved by developing prediction models of those output parameters in terms of the input parameters with the help of statistical analysis tools. Correlation analysis will also be performed in order to map the nature of relationships among the all types of parameters, which describe and affect the weld. Another objective is to find the optimal settings for GMAW with metal cored wires, which satisfy the required specifications of VCE. Moreover, this project aims at investigating the possibility of increasing productivity when using metal cored wires. Finally, the effect of pulsed welding on the output parameters will be examined and measured.

## 1.3 Problem analysis

Being able to control the welding process is critical in order to achieve specific quality requirements in GMAW. For fatigue loaded welded joints, having a deep penetration and large toe radius is usually more important than having a large throat thickness. Since measuring the penetration depth with non-destructive techniques is not an easy process, it is a common practice that penetration is controlled through the welding parameters. Even though there

is a general knowledge on the connection between welding parameters and dimensions, more research is needed in order to be able to predict the weld final shape (Hammersberg, & Olsson 2013).

Moreover, new production processes and new consumables have come to surface such as pulsed current and metal cored wires, respectively. As it is evident from (Hammersberg, & Olsson 2013), while using solid wires, geometrical parameters can compensate for bead geometry losses when productivity process variables are optimized for GMAW. Nevertheless, little research is performed on the combined effects of selected productivity and geometrical parameters on weld dimensions when using metal cored wires and pulsed welding.

Therefore, the main research questions for this thesis project are:

- 1) What is the influence of selected productivity and geometrical parameters on weld dimensions?
- 2) What are the correlations among all input and output parameters?
- 3) What is the optimal combination of geometrical parameters for higher weld quality?
- 4) Having set the optimal values for geometry parameters, is it possible to enhance productivity through increased travelling speed?
- 5) How does pulsed welding affect the output parameters?

#### 1.4 Delimitations

Delimitations for this thesis project are:

- This project will only consider robotized GMAW of fillet welds with solid and metal cored wires produced at Elga AB
- Waist plates of mild steel with a prepared edge and a thickness of 6mm will only be used. Flange plates with thickness of 10 and 12mm will be used
- Welding will only be performed using a Miller NX 100 ERCS-EA1400NAE00 power source with the following characteristics: AC 400/415/440, Average 1.8kVA, Power supply peak 3.3kVA
- Welding will only be performed using the robot Motoman by YASKAWA
- Welding will only be made using argon (80%) and CO<sub>2</sub> (20%) as shielding gases
- Measurement of the welds will be performed only through Lumenera software
- Analysis of the weld measurement data will only be carried out through JMP11 software



- Penetration in both plates, toe radii, leg lengths and bead thickness will only be measured as response variables



## 2. Theory

### 2.1 GMAW

Gas metal arc welding (GMAW) is very widely used in many industrial areas since 1948, when it was firstly used for aluminium welding. The process is widely referred also as MIG (metal inert gas) or MAG (metal active gas), depending on if the used shielding gas is inert, such as argon or if it contains also active gas, such as CO<sub>2</sub>. The principle of GMAW operation can be described through the following picture.

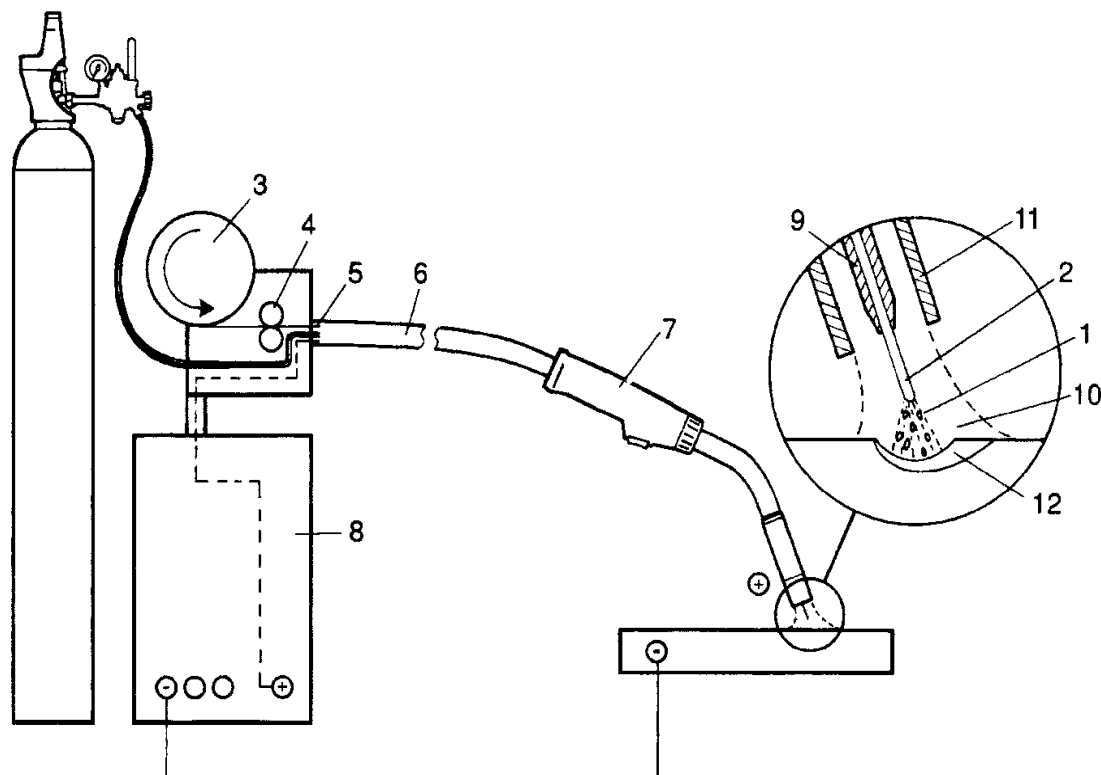


Figure 1 GMAW principle (Weman 2011)

The metal wired electrode (2) is fed from a reel (3) to the welding gun (7) with the help of the drive rollers (4). Before the wire reaches the gun, it is driven through a conduit (5) and the hose package (6). The contact tube (9) inside the welding gun, which usually connects to the power source's positive pole, is the mean through which, electrical energy is transferred to the wire. The arc (1) is created between the wire and the workpiece, which is connected to the negative pole of the power source (8), and the circuit is completed. Finally, the shielding gas (10), which is supplied through the gas nozzle (11), prevents from oxide formation and protects both the arc and the weld pool (12) (Weman 2011).

GMAW has many advantages such as high deposition rates and welding speeds, little post weld cleaning, as well as wide applicability in many types of metals or alloys and for high number of welding positions. These benefits have enhanced the automation and robotization of the process, for increased productivity, quality and precision (O'Brien 1991)

In the recent years, many developments have been achieved in GMAW, such as digital control of power sources for more regularized metal transfer and introduction of new consumables for more stabilized weld pool (Weman 2011).

### *2.1.1 GMAW parameters*

Understanding and modelling the complex relationship between process parameters, weld bead geometry and quality in GMAW has been a challenging task since the mid 1900s (Karadeniz et al 2007). The difficulty of this task arises due to the fact that in GMAW, physical, chemical and mechanical phenomena take place in the same time, while all states of matter interact in a very short area at high temperatures (Ramos-Jaime et al 2013).

In general, GMAW process is controlled by a set of welding parameters, which can be divided into productivity and geometrical parameters (Weman 2011).

#### *2.1.1.1 Productivity parameters*

Welding current is one of the main welding productivity parameters, which can affect weld quality and is usually determined according to plate thickness and travelling speed (welding process handbook). It is found that its relationship with wire feed rate is linear for low values, and non-linear for higher values of current, when all other parameters remain constant (O'Brien 1991).

Regarding electrode diameter, the larger it is, the more current is required for the welding process and therefore, deposition rate and penetration increase as well (welding handbook). It is also observed that welding with a smaller electrode diameter can produce smoother material transfer (Weman 2011).

Voltage is a productivity parameter directly related to arc length and affects how wide the weld bead is. It is dependent on arc length, type and diameter of electrode, as well as on shielding gas (O'Brien 1991).

Travelling speed determines how fast the arc is moving along the joint. If the travelling speed is very low, penetration decreases and weld bead widens. In contrast, when it is very high, the heat per unit length and the deposition rate of the filler metal decrease, therefore undercutting is a common defect (O'Brien 1991).

Moreover, electrode stickout refers to the distance from the contact tube to the edge of the wire. Having a long stickout during GMAW can increase the

electrode resistance and consequently the voltage drop between the contact tube and the work-piece. As a result, the current, melting rate and arc length are decreasing (O'Brien 1991). On the other hand, choosing a very small electrode stickout can lead to burn-back, which happens when the wire is welded with the contact tube (Weman 2011).

Inductance, another process parameter has an important role in determining the welding properties in GMAW. When inductance is low the arc is more concentrated but produces more spatter. A softer result and a wider bead can be achieved with an increased inductance. On the other hand, a very high value of inductance can decrease the arc stability and lead to stubbing (Weman 2011).

Additionally, the shielding gases used in GMAW, depending on the material to be welded can be inert (Argon, Helium), active (CO<sub>2</sub>), or a mixture of these two types (O'Brien 1991). The gas flow rate of the gases used in each application is determined by the value of current used and by the type of material to be welded (Weman 2011).

#### *2.1.1.2 Geometrical parameters*

Geometrical parameters refer to all the parameters related with to the exact position of the torch and the plates during welding. As far as torch angles are concerned, it is generally observed that pushing the weld gun creates shallower and wider weld geometry, while pulling creates a deeper and narrower profile. Regarding the angle between torch and working piece (horizontal position), it is usually set at 45 degrees in order to achieve a more uniform result (O'Brien 1991). Besides the two angles described above, there is a variety of other geometrical parameters which affect GMAW quality such as waist plate angle, the slope (up or down), the slit (gap) between the plates and the welding position (Hammersberg, & Olsson 2013).

#### *2.1.2 GMAW Consumables*

GMAW consists of process consumables, which are filler materials (electrodes) and shielding gas. Importance of consumables in GMAW process lies on the fact that geometry of the weld is determined by the appropriate choice of these consumables, which in turns determines mechanical properties of it. Selection of process consumables is influenced by several factors such as welding position, required mechanical properties and base metal. Suppliers provide assistance in choosing the appropriate filler material for every application which can come from a list of solid or cored wires (O'Brien 1991; Weman 2011).

##### *2.1.2.1 Solid electrode*

Solid wires are the most commonly used electrodes in MIG/MAG welding. They can be spooled or reeled in order to have a continuous feeding of the

gun. Wires are relatively small compared to other techniques of welding such as submerged arc welding with diameters ranging between 0.9 – 1.6 mm although wires as small as 0.5 mm and as large as 3.2 mm exist in a few industrial applications (Davis 2009; O'Brien 1991; Weman 2011). Solid wires can be applied to weld several types of materials such as mild steel, low alloyed and stainless steels, aluminium, nickel and copper alloys. Solid wires usually have similar chemical composition with the base material and they are often coated with copper to improve productivity (Weman et al 2006).

#### 2.1.2.2 Cored wire

Another type of electrodes which use is rising over the years is cored wires. These electrodes consist of a metallic sheath covering a powder-metal core (metal-cored wires) or a core filled with flux (flux-cored wires), as presented in Figure 2.

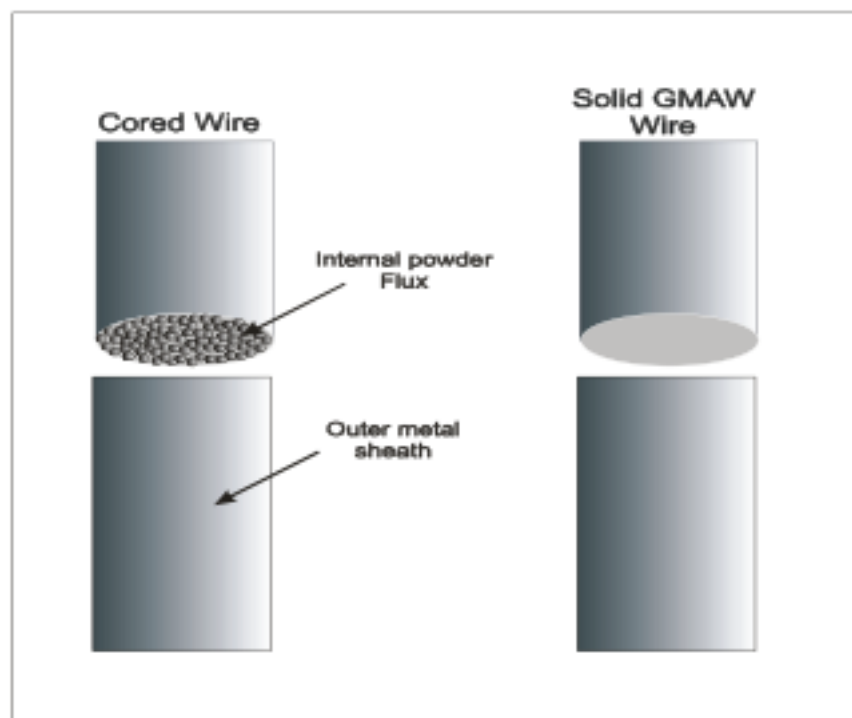
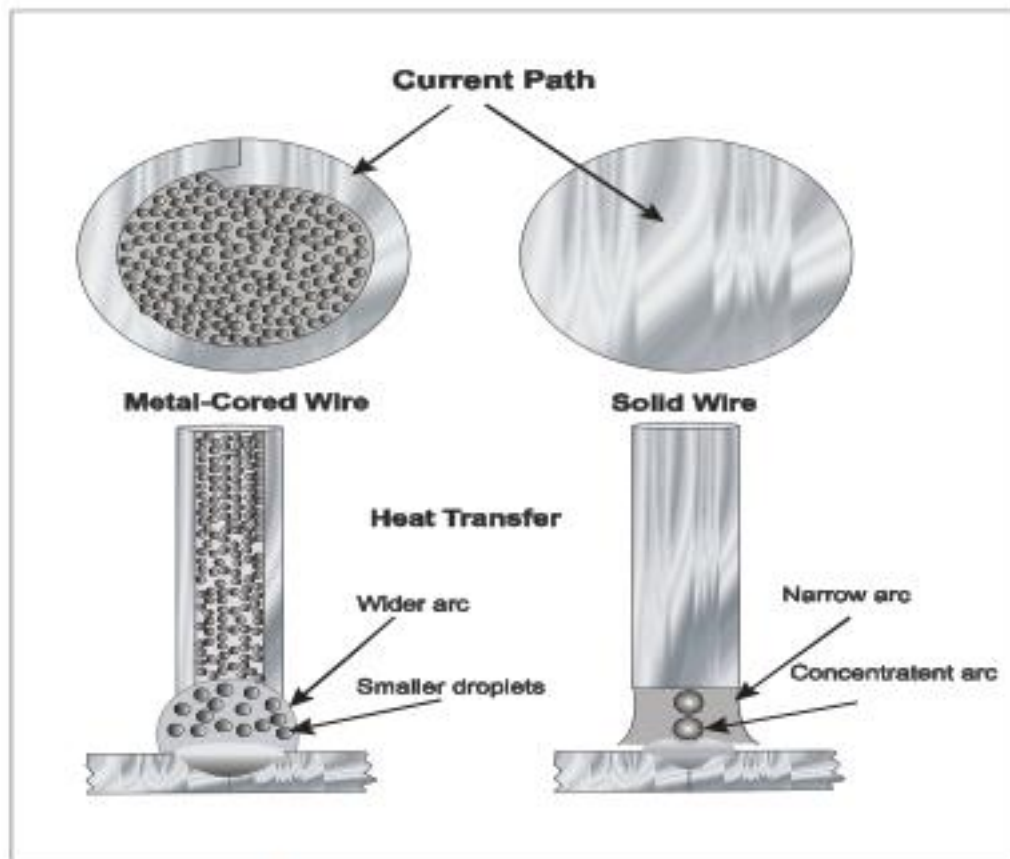


Figure 2 Overview and section of cored filler and solid wire

These wires can be used for a wide variety of materials and thicknesses with the same success as solid wires. The availability of suppliers to modify the composition of the core allows industries to produce and customize the wires according to any requirements and specifications needed (Liao, & Chen 1999; Ibrahim et al 2012). The same equipment of solid wires with the restriction of using only U-shaped feeding roll can use these wires. The only actual difference is that cored wires often need water-cool welding gun (Weman et al 2006).

Comparing arcs between wires as it is seen in Figure 3 cored wires appear to have wider arcs with smaller droplets at the same time. On the other hand, solid wires have a more concentrated and narrow arc (Weman et al 2006).



**Figure 3 Schematic differences between cored and solid arcs**

Nowadays, cored wires have substituted solid wires in a large extent due to its significant benefits listed below:

- High deposition rates. Up to 20% higher than with solid wire
- Increased travelling speeds
- Less spatter minimizing silicon islands.
- Variance of the alloying constituents depending on the application
- Less lack of fusion
- Better sidewall melting
- Less pre or post weld processes, therefore reduced required time for completion of a weld leading in higher productivity (Liao, & Chen 1999; Davis 2009; Weman 2011)

However, it has to be mentioned that cored wires show some important drawbacks:

- Higher price for cored wires but not necessary higher total cost of production
- Difficulty in finding the perfect values for parameters
- Restricted current ranges for satisfactory welding (Liao, & Chen 1999; Davis 2009; Weman 2011).

Over the last years metal cored wire outperforms the flux cored because of its superior properties especially in horizontal welding position and its reduced lead times (Kuvini 1998).

Analytically the advantages with the use of metal cored wires instead of flux cored are:

- Reduced fume production
- Higher deposition rates and efficiency
- Improved penetration
- Less slag and spatter
- Silicon islands in the centre of the bead where they are easily removed (Weman et al 2006; Kuvini 1998; Weman 2011)

### *2.1.3 Welding Technology*

GMAW is used in a wide variety of ferrous and non-ferrous metals such as mild steel, aluminium, stainless steel nickel alloys etc. and on plate thicknesses down to 0.7 mm. On the same time industrial applications require attractive and quality welds. In order to achieve this need for a variety of materials and different thicknesses, consistent and complicated procedures are required to stabilise the arc in each case (Weman 2011).

#### *2.1.3.1 Metal Transfer*

Stability of an arc is highly dependent on the metal transfer from the electrode into the welded material. For different values of current and voltage, different arc types appear as seen in Figure 4 (Weman 2011).

Globular metal transfer appears at low currents. In that transfer mode big droplets are created and gravity is the driving force for detachment into the weld pool (Iordachescu, & Quintino 2008).

At relatively low voltage short arc welding dominates. Both globular and short arc transfer modes have low heat input which makes these processes suitable for thinner materials. However, lack of control of droplets and arc in the case of globular transfer and spattering due to low inductance in short circuiting bridge of molten metal, make these transfer modes not applicable when high quality welds are needed (Praveen et al 2005).

Spray arc welding, which is stable and spatter free is applied at high values of current and voltage. Deposition rates are high, but large pools, high heat input



and only “downhand” possibility to perform welding are some of the drawbacks in this transfer mode (Palani, & Murugan 2006; Praveen et al 2005; Weman 2011).

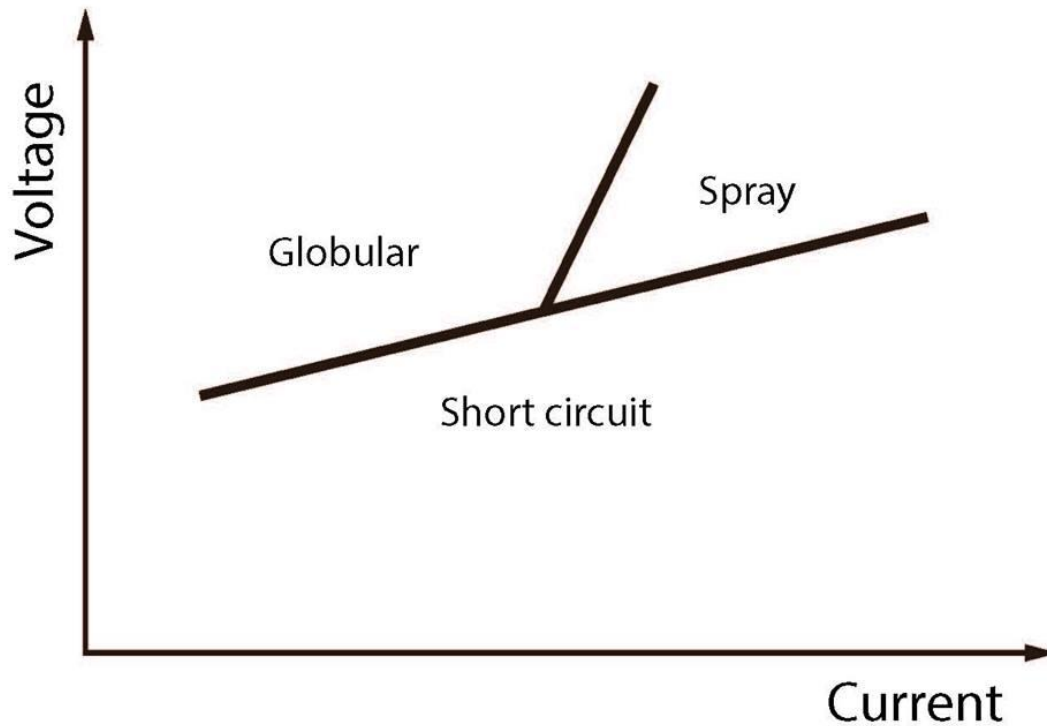


Figure 4 Transfer modes for different current and voltage

#### 2.1.3.2 Pulsed Technology

During 1960s' a new alternative method of welding was developed called pulsed welding. This metal transfer mode uses current pulses in order to control the droplets of the electrode in the arc, creating a stable and spatter free arc (Praveen et al 2005; Weman et al 2006). As a consequence, pulsed welding expands the current range of spray welding in lower values. Since the heat input of pulsed MIG process is relatively low, this technique is suitable for thinner materials, substituting short circuiting and globular transfer mode (Weman 2011). Current in pulsed GMAW is varied periodically between a minimum value (background current) and a maximum value (peak current), in a way that the mean value of current never exceeds the level of spray arc welding (Praveen et al 2005). The purpose of the pulse is to supply the necessary heat by adding the right amount of current to melt the filler material and detach a single droplet for every pulse (Figure 5). Unlike conventional welding, pulsed welding reduces the current when extra heat is not needed, causing a technical cooling (Praveen et al 2005; Weman 2011).

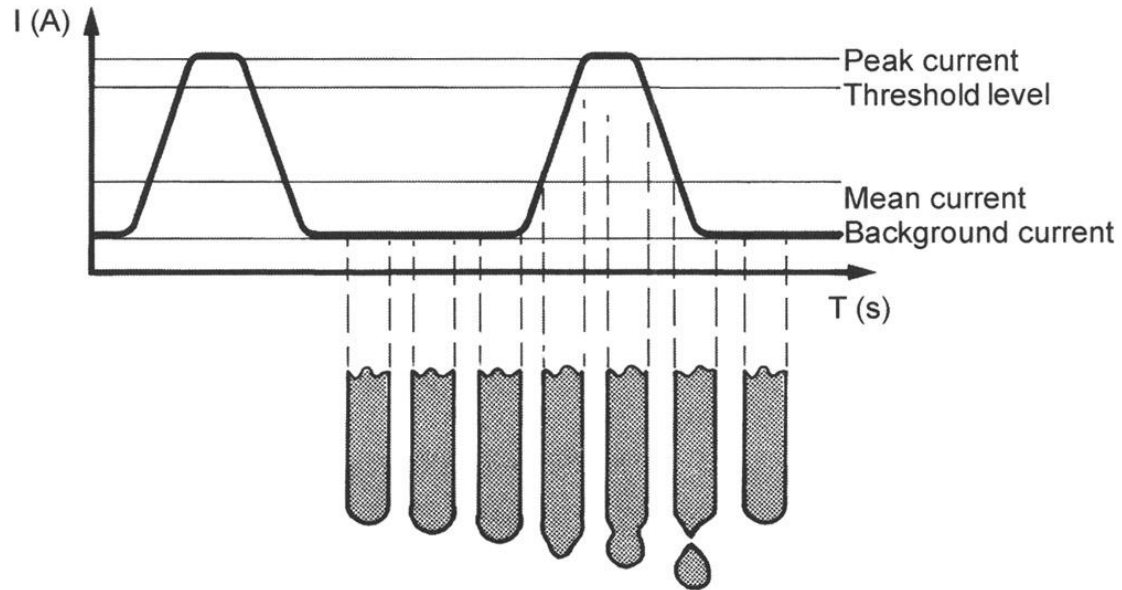


Figure 5 Pulsed welding and the way electrode melts (Weman et al 2006)

Aluminium, stainless and mild steels are commonly welded with pulsed GMAW either with solid or cored wires (Weman 2011). More specifically, cored wires combined with GMAW-P show significant advantages compared with conventional welding due to the range where cored wires are most effective. Better penetration, proper bead appearance, high deposition rates and availability to use an increased electrode diameter are some of the advantages by using pulsed welding (Palani, & Murugan 2006; Praveen et al 2005; Weman et al 2006; Weman 2011).

## 2.2 Statistical analysis

### 2.2.1 Linear regression

Regression analysis is a very common statistical approach, which is widely used in order to perform analysis of data obtained from designed experiments. Least square linear regression is the most common type of regression used in order to estimate the value of a dependent variable from the value of a single independent variable (linear regression), or more independent variables (multiple linear regression). In detail, the approach is described by the equation:

$$Y = b_0 + b_1X_1 + b_2X_2 + b_3X_3 + \dots + b_kX_k + \varepsilon \quad (\text{Ryan, 2000})$$

In this model,  $Y$  represents the dependent variable and  $X_1, X_2, \dots, X_k$  are the independent variables. Constant  $b_0$  is the intercept of the model, while the coefficients  $b_0, b_1, \dots, b_k$  are the regression coefficients and represent the slope for  $X_1, X_2, \dots, X_k$  respectively. The  $\varepsilon$  is an error term which symbolizes the nature of the inexact relationship between  $X$  and  $Y$ . An assumption for

using multiple regression analysis appropriately is that errors are independent and normally distributed (Ryan, 2000).

### 2.2.2 Scatter plot and correlation analysis

Scatter plot is a graphical tool, used in order to describe the relationship between two variables. It is more common that the vertical axis of a scatter plot refers to the dependent variable, while the independent variable is placed on the horizontal axis. Points on the scatter graph represent the pairs of data. Moreover, the way these points are distributed in the graph is an indicator of the degree and type of correlation that exists between the dependent and independent variable. A straight line connecting all the points of a scatter plot represents the perfect correlation between two variables. In general, as it is presented in Figure 6, scatter plots can reveal four types of patterns; positive, negative, curvilinear correlation or no correlation at all (Jackson, 2008).

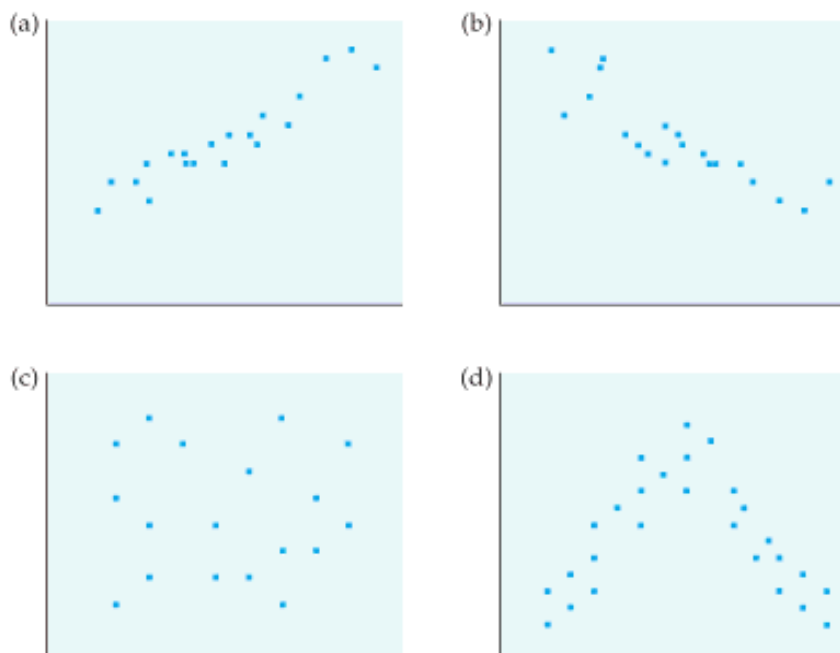


**Figure 6 Possible types of correlational relationships: (a) positive, (a) negative, (c) none, (d) curvilinear (Jackson, 2008).**

When positive correlation exists, an upturn in one of the two variables is related with an upturn of the other one. In contrast, when a decrease in one variable is connected with an increase in the other variable, negative correlation between the two variables exists. In general, correlation analysis is helpful in order to measure linear relationships between variables. When a relationship between two variables is curvilinear, a pattern in the data cannot be accurately and adequately indicated by a correlation coefficient (Jackson, 2008).

In addition, in order measure the degree of linearity in variable relationships, the Pearson product-moment coefficient is widely used. This correlation

coefficient can be calculated as  $r = \frac{\sum (x - \bar{x})(y - \bar{y})}{\sqrt{\sum (x - \bar{x})^2} \sqrt{\sum (y - \bar{y})^2}}$ , where X and Y are

the two response variables whose relationship is examined. The coefficient can get values from -1 (perfect negative correlation) to 1 (perfect positive correlation). Deciding on the ranking of the correlation size is necessary in order to interpret coefficients and depends on the context of the study being carried out (Jackson, 2008).

### 3. Experimental Process

#### 3.1 Welding process

This chapter describes the methods and procedures involved in performing and analyzing the experiments.

All welding experiments, sample preparations and measurements were carried out at Elga AB facilities and laboratories.

The experimental process was held in several steps:

- Step A (solid wires): In order to verify results from previous research done in cooperation with VCE, 3 experiments with solid wire were repeated with the same settings
- Step B: 16 experiments with a wire feed speed of 8.5 m/min were performed by varying gun angles and welding position
- Step C: 16 experiments with a wire feed speed of 9.5 m/min were performed by varying gun angles and welding position
- Step D: 4 selected experiments from the previous steps were repeated at four different higher travelling speeds and a higher wire feed speed
- Step E: 12 selected experiments from all the previous steps were repeated in pulsed welding

##### 3.1.1 Welding Parameters

Regarding Step A, a previous research carried out by Hammersberg & Olsson (2013) was taken under consideration in order to test consistency of both GMAW robots in VCE and Elga AB. Three experiments were repeated with productivity settings, which were set in cooperation with VCE. The productivity parameter values for Step A are presented in Table 1.

Considering Step B, since metal cored wire behaves differently than solid electrode a lower value of wire feed rate and voltage was suggested from Elga AB (Table 1). Moreover, geometrical parameters and welding fixture were varied at different values as seen below in Table 2. The parameters are explained graphically in Figure 7.

Table 1 Productivity parameters used in all steps

	Wire	Voltage (V)	Wire Feed rate (m/min)	Welding Speed (cm/min)	runs
Step A	Solid	29,5	15	48	3
Step B	Metal cored	28,7	8,5	48	16
Step C	Metal cored	29,8	9,5	48	16

<b>Step D</b>	Metal cored	31	12	60/65/70/75	16
<b>Step E</b>	Metal cored	25,5	8,5/9,5/12	48/50/70/75	12

Table 2 Geometrical parameters

Parameters	Value 1	Value 2
Gun angle X	35°	45°
Welding direction	Push	Pull
Angle Y	60°/75°	105°/120°
Welding position	PB (90°)	PA (45°)

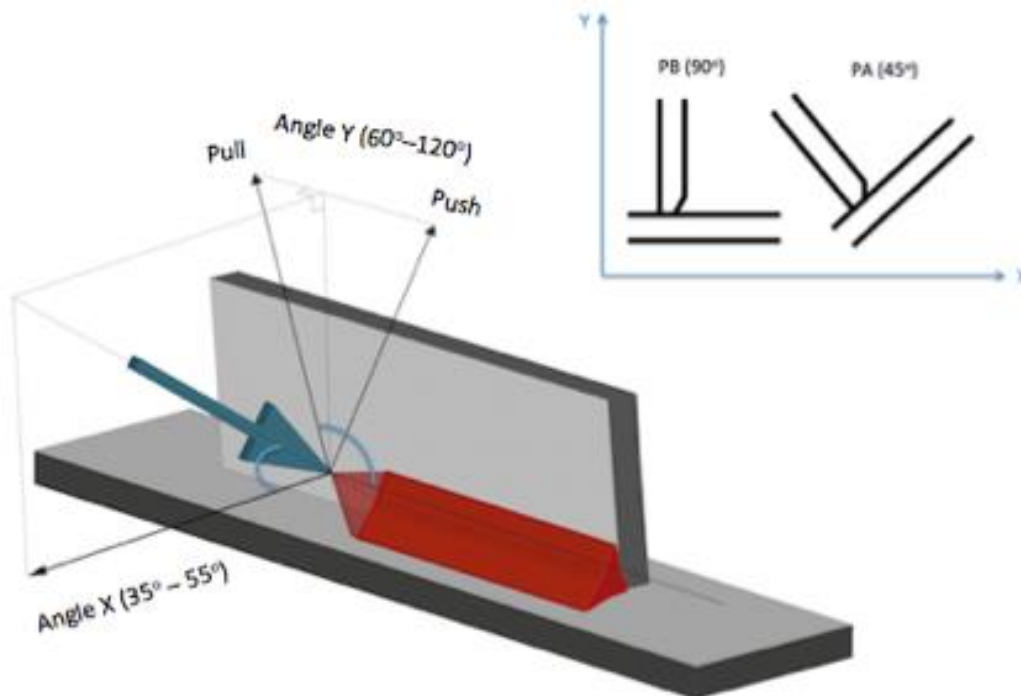


Figure 7 Geometrical parameters illustrated in a fillet weld as measured for experimental process

During experiments in Step C wire feed rate was increased at 9.5 m/min and voltage 29.8 Volts. All possible combinations of geometrical parameters presented in Table 2 were reproduced.

As far as Step D is concerned, higher productivity was put in focus. In particular, the best two welds one from push direction and the other from pull were selected from step B and repeated. Another pair of experiments was selected in the same manner from step C. The combination of productivity parameters for Step D is shown in Table 1.

Finally, pulsed welding (Step E) was performed for the four welds with the higher quality from step B, step C and step D consequently applying the exact

same settings used in those runs. The target in this step was to compare pulsed with conventional welding with different productivity settings and depict drawbacks and benefits of each type of welding.

In total 63 experiments were conducted and analyzed. These experiments can be found in Appendix A.

### 3.1.2 Base Material

As base material for welding mild steel plates of 6mm, 10mm and 12 were used. The flange plates which were used had a thickness of 10 or 12mm and the waist plates had a thickness of 6mm and a prepared edge (Figure 8).

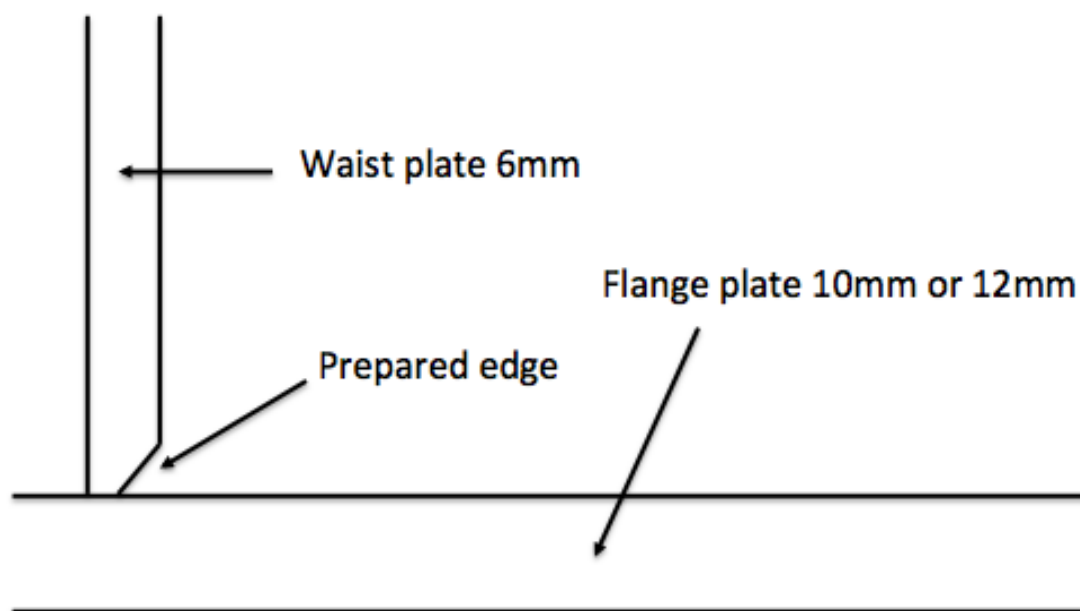


Figure 8 Fillet structure with base material

### 3.1.3 Robotic welding

All experiments were performed using robotic technology. A robotic system consists of three parts:

- 1) Arc robot
- 2) Power source
- 3) Gas system

Elga's facilities use Motoman YASKAWA as an arc robot seen in Figure 9.

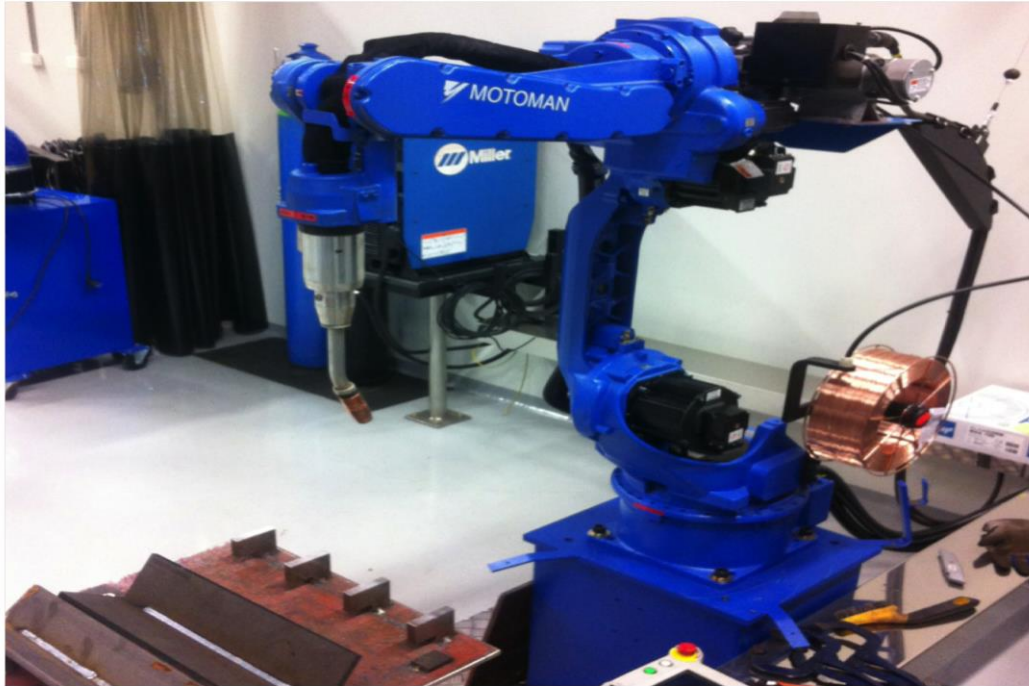


Figure 9 Arc robot – Motoman

Power source is a Miller NX 100 ERCS-EA1400NAE00 with characteristics: AC 400/415/440, Average 1.8kVA, Power supply peak 3.3kVA (Figure10).



Figure 10 Power Source - Miller

Premixed gas system used for the experiments consisted of 80%Ar+20%C (Figure 11).





Figure 11 Gas system

### 3.1.4 Electrodes

During this experimental process two certain types of filler materials were used.

Initially, Elgamatic 100 was used for the first three experiments (Step A). This is a mild steel wire coated with copper, which is suitable for general engineering applications and automated welding systems as well. Its composition and mechanical properties are presented in Table 3 and Table 4.

Table 3 Elgamatic 100 – Solid Wire. Wire composition, wt%

	<b>C</b>	<b>Si</b>	<b>Mn</b>	<b>P</b>	<b>S</b>	<b>Cu</b>
Min	0,07	0,80	1,40			
Typ	0,08	0,85	1,45	0,010	0,015	0,05
Max	0,12	1,00	1,60	0,025	0,025	0,35

Table 4 Mechanical Properties of Elgamatic 100

	<b>Typical</b>
Yield Strength	470 MPa
Tensile Strength	550 MPa
Elongation	26%
Impact Energy	-20 °C x 85 J

Concerning the other 60 experiments and the core of this study, Elgacore MXA 100 wire was used. This is a metal cored wire suitable for flat and horizontal-vertical positions. Deep penetration, low level of spatter and absence of slag are its most significant advantages. Lastly, Elgacore MXA 100 is suitable for robotic welding. Its composition and mechanical properties are presented in Tables 5 and 6.

Table 5 Elgacore MXA 100 – Cored wire. Wire composition, wt%

	<b>C</b>	<b>Si</b>	<b>Mn</b>	<b>P</b>	<b>S</b>	<b>Cr</b>	<b>Ni</b>
Min							
Typ	0,05	0,75	1,55	0,011	0,009		
Max	0,12	0,90	1,75	0,03	0,03	0,20	0,50

Table 6 Mechanical Properties of Elgacore MXA 100

	<b>Typical</b>
Yield Strength	460 MPa
Tensile Strength	555 MPa
Elongation	30%
Impact Energy	-40 °C x 80 J

Elga AB supplied those two electrodes described above, which are typically used in the market.

### 3.2 Sample preparation

Next step after completion of welding experiments was to prepare the samples for measurement. Small cross sections of the welds were created by a cutting machine (Figure 12). The dimensions of each piece were approximately in the range of 1.2cm x 1.2cm x 4cm.



Figure 12 Cutting machine

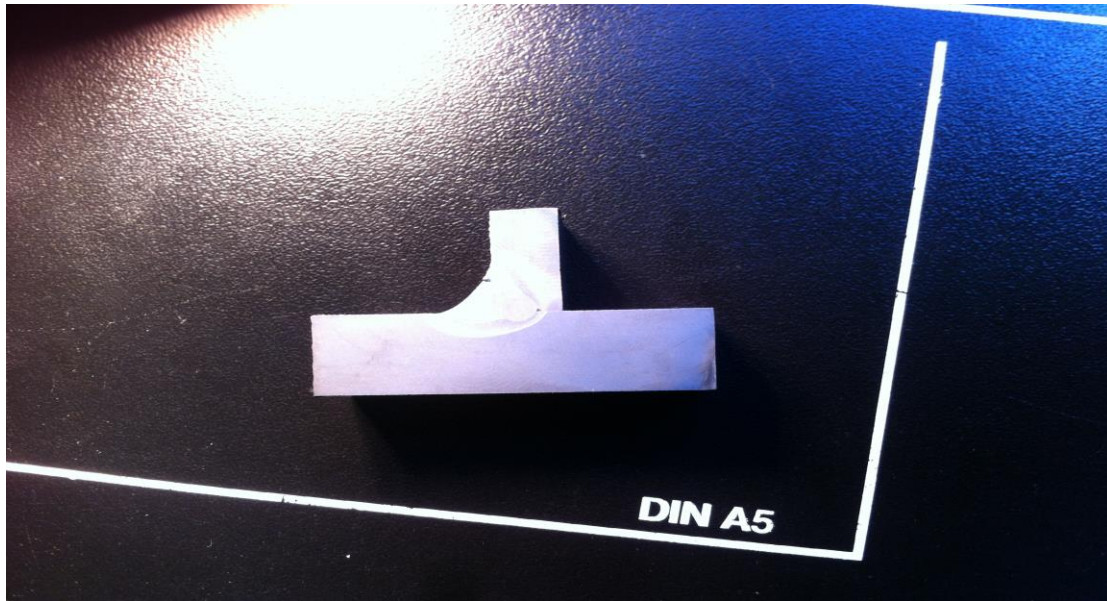
After cutting, samples were grinded with SiC papers of several grits (Figure 13) until they acquired a smooth surface.



Figure 13 Grinding machine

Lastly, samples were etched using nitric acid in order to reveal the welded area and its microstructure (Figure 14).





**Figure 14 Grinded and etched sample**

### 3.3 Measurement

Weld geometry of each sample was measured via Lumenera software (Figure 15). Each sample was captured and by using the software's tools, all dimensions of the weld such as leg lengths, penetration and toe radii were measured as shown in Figures 16 and 17.



**Figure 15 Lumenera Measurement System**

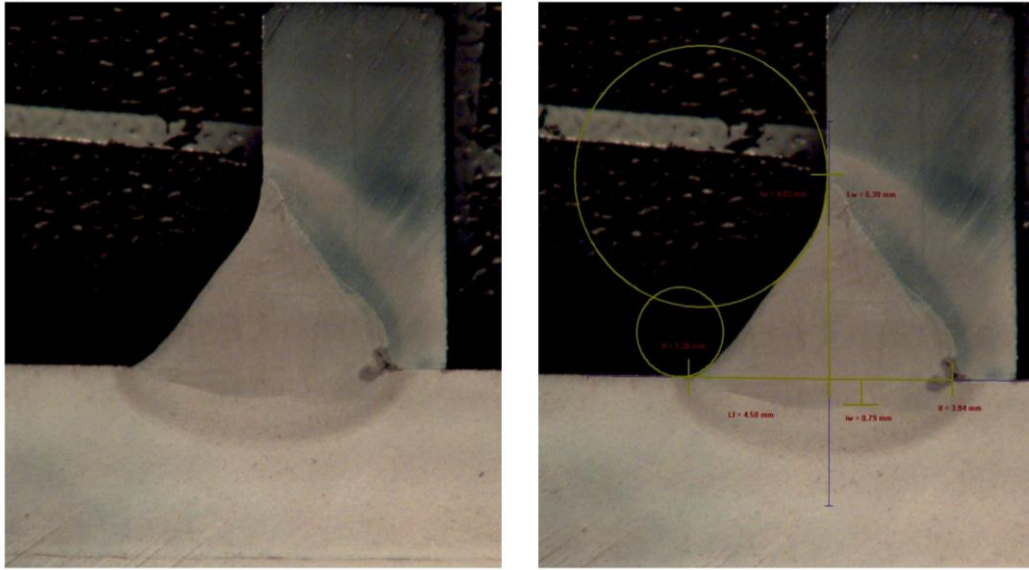


Figure 16 Sample's weld dimensions measurement via Lumenera Software

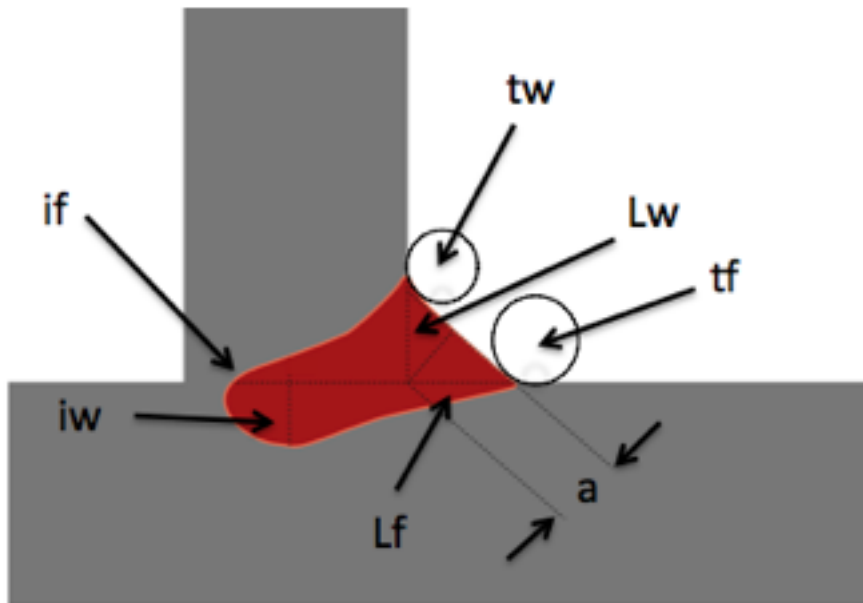
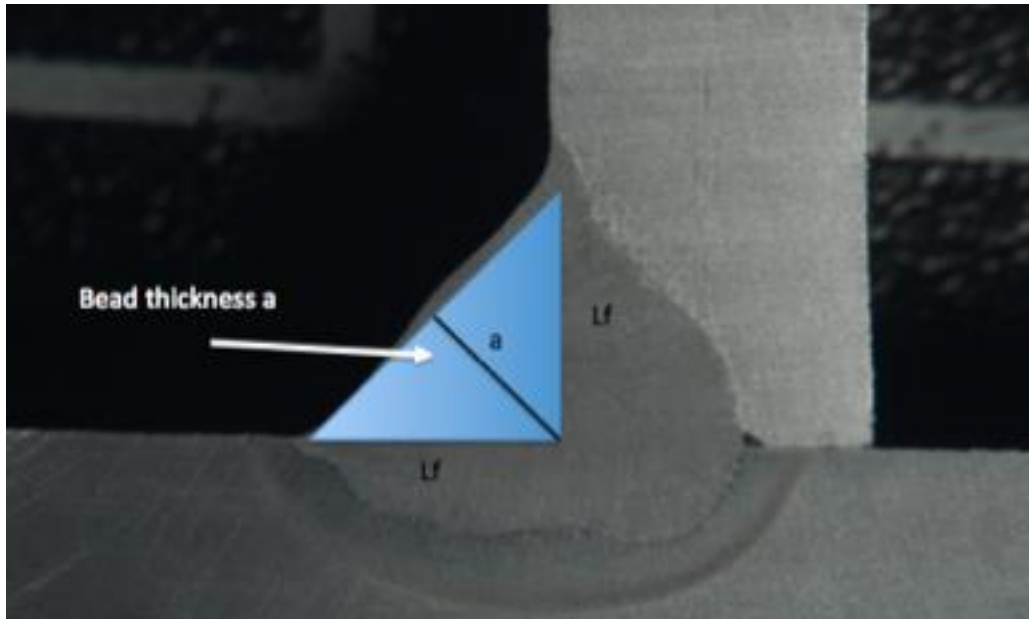


Figure 17: Measurement of the response variables

The bead thickness was determined by drawing an equilateral triangle, as shown in Figure 18. Each vertical side of this triangle is equal to the shortest leg length ( $L_f$  or  $L_w$ ) and the bead thickness is equal to the height of this triangle. The process explained above is described by the following equation:

$$a = \frac{\sqrt{2}}{2} L$$



**Figure 18: Measurement of bead thickness**

### 3.4 Statistical Analysis

Analysis of the measurements was carried out by JMP 11 Software package by SAS. The prediction models connecting input and output parameters were constructed by using the standard least square regression. Bar charts, distribution charts and scatterplots were also produced in order to process and visualize the obtained welding data. Regarding correlation analysis, the correlation coefficients were calculated by JMP11 using Pearson's formula, which is presented in Chapter 2.

## 4. Results

### 4.1 Step A

Results from that step are shown in table 7. Test runs S1, S2, S3 were performed as a reference to three experiments selected from the previous work of Hammersberg & Olsson (2013). All experiments in Step A are presented in Appendix A. The three welds which were performed showed a 30% higher penetration in the flange plate and a 35% smaller bead thickness in comparison to the previous identical tests conducted by Hammersberg & Olsson (2013).

Table 7 Response parameters measurements

Test run	tf	tw	if	iw	a
<b>S1 ref. test 1</b>	0,68	1,2	<b>6,78</b>	4,1	<b>3,42</b>
<b>S2 ref. test 2</b>	0,36	1,47	<b>4,47</b>	2,67	<b>4,04</b>
<b>S3 ref. test 3</b>	0,72	1,39	<b>3,77</b>	3,13	<b>4,12</b>
<b>Test 1</b>	0,85	4,2	<b>5,39</b>	4,66	<b>5,07</b>
<b>Test 2</b>	0,5	4,7	<b>3,47</b>	3,17	<b>5,5</b>
<b>Test 3</b>	1	2,75	<b>3,1</b>	2,98	<b>5,42</b>

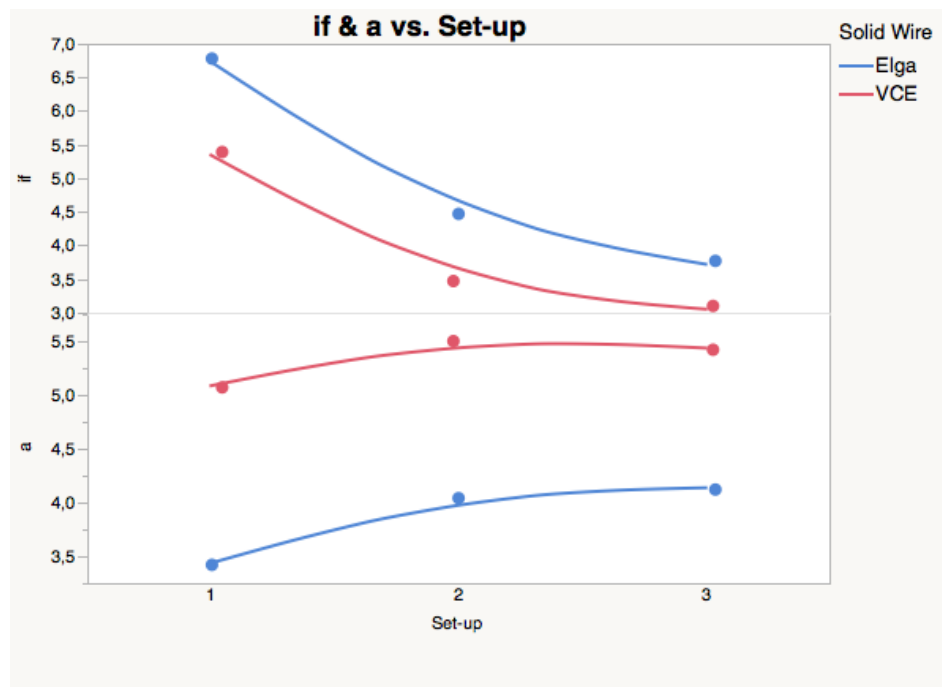


Figure 19 Response parameters illustrated graphically for Step A

## 4.2 Step B & C

### 4.2.1 Mean values and standard deviations

The mean values of all the response variables for both steps B and C were plotted in order to perform a comparison between the two wire feeds of 8.5 and 9.5 m/min. The results, which are presented in Figure 20, show that all the response parameters have higher average values when wire feed rate is 9.5 than when it is 8.5 m/min. In other words, more high quality welds in total are produced in Step C than in Step B.

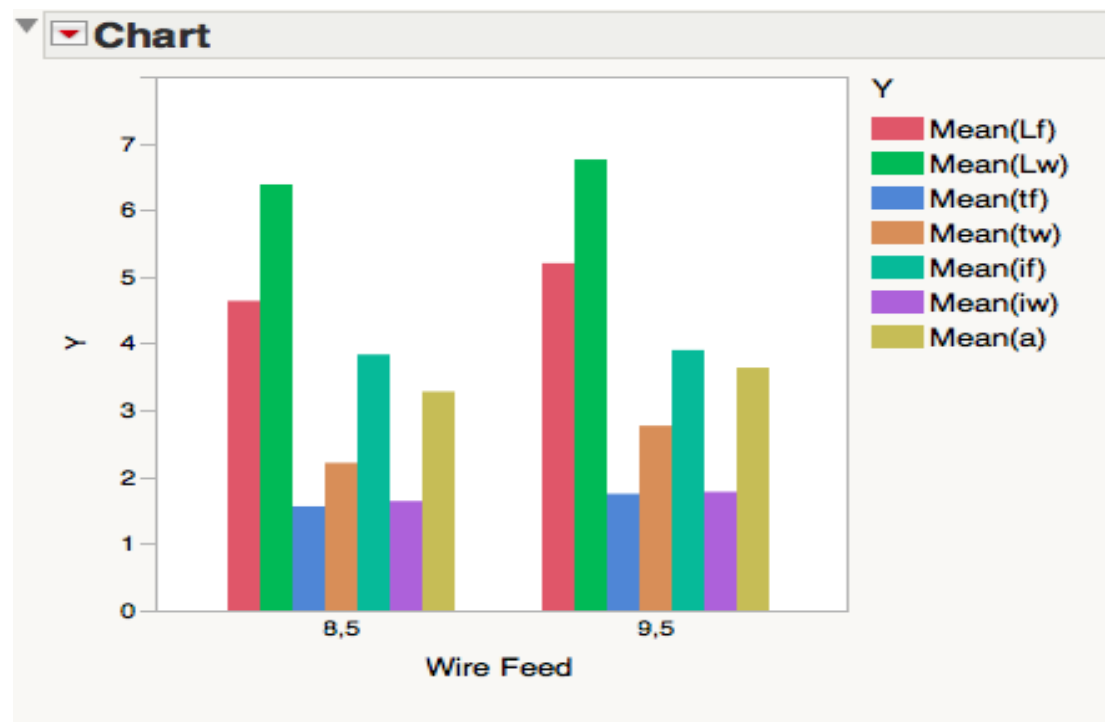


Figure 20 Mean values of response parameters in Steps B & C

In order to grasp a more descriptive image of how the data differ in Steps B and C, the standard deviations of the response parameters were plotted and compared, as it is shown in Figure 21.

In contrast with Figure 20, it is evident that welding in step C produces more variation for all response variables than in Step B.



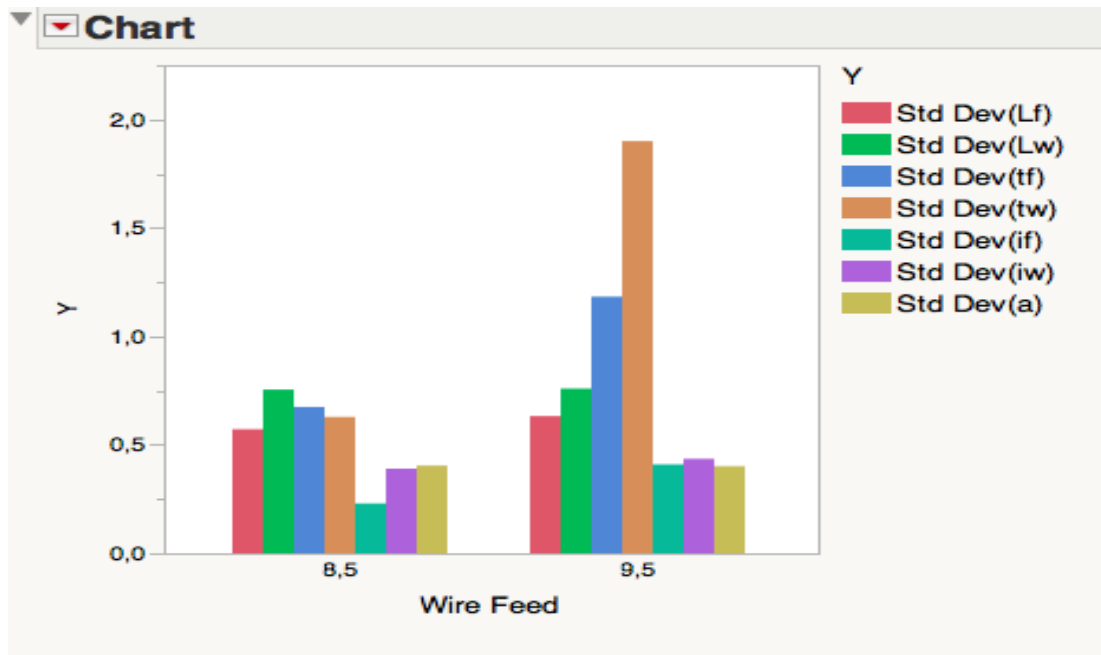


Figure 21 Standard deviations of response parameters in Steps B & C

#### 4.2.2 Distributions

In order to investigate which welding settings correspond to the most acceptable welds, distribution charts were plotted from the obtained data. After discussions with VCE, lower limits were set for the most important response variables:

- $if \geq 2\text{mm}$
- $iw \geq 1\text{mm}$
- $tf \geq 1\text{mm}$
- $tw \geq 1\text{mm}$
- $a \geq 3\text{mm}$

In general, a maximization of all the above variables was considered to be desirable from a quality perspective. A weld was therefore perceived as acceptable if it satisfied the above requirements. The distribution charts (Figure 22 and 23) showed that the highest percentage of acceptable welds in Steps B and C was performed in the “push” welding direction at a gun angle of 35 degrees and in the PA welding position (45 degrees).

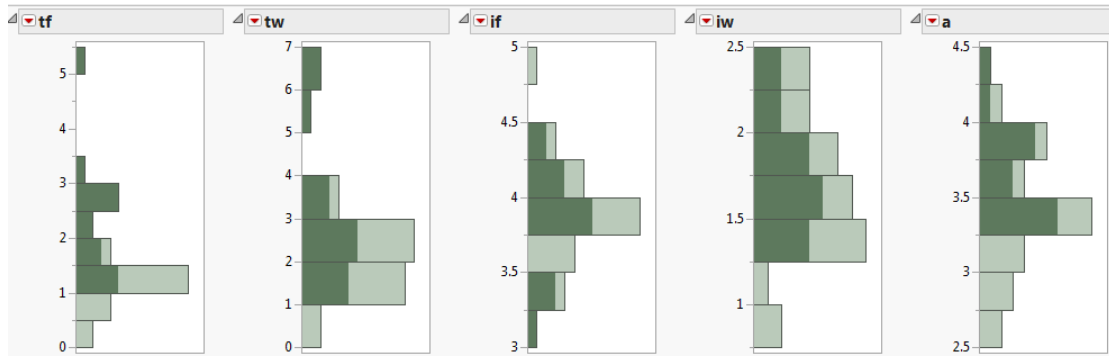


**Figure 22** Distribution of main response parameters for Steps B & C. Dark green area represents the selection of the accepted values of the parameters



**Figure 23** Distribution of input parameters for steps B and C. Dark green area corresponds to the welds that fulfill all requirements

#### 4.2.3 Bivariate relationships

The relationships among all the response variables were investigated by constructing scatterplots matrices in JMP 11 software. In Figure 25 the scatterplot matrix corresponding to Step B is presented. By observing the correlation coefficients matrix (Figure 24), conclusions can be drawn regarding bivariate relationships. Regarding the ranking and interpretation of the correlation coefficients, the following scale was used in order to define the degree of correlation in each case:

- $0 \leq r \leq 0.29$ : no correlation
- $0.3 \leq r \leq 0.59$ : low positive correlation
- $0.6 \leq r \leq 0.79$ : moderate positive correlation
- $0.8 \leq r \leq 0.99$ : strong positive correlation

The same scale applies for negative correlations with the difference of using negative values for coefficients. The correlations among variables for Step B can be summarized in the following points:

- 1) Low positive correlation
  - tw and Lw
  - if and Lw
  - tf and Lf
  - iw and Lf
  - if and tw
  - tf and if
  - a and iw
  - a and tf
- 2) Low negative correlation
  - Lw and Lf
  - a and Lw
  - iw and if
- 3) Moderate negative correlation
  - Lw and iw
- 4) Strong positive correlation
  - Lf and a

Multivariate							
Correlations							
	Lf	Lw	tf	tw	if	iw	a
Lf	1.0000	-0.3207	0.4156	0.1160	-0.1578	0.4979	1.0000
Lw	-0.3207	1.0000	0.0498	0.5071	0.5181	-0.6731	-0.3206
tf	0.4156	0.0498	1.0000	0.2520	0.4884	-0.1192	0.4151
tw	0.1160	0.5071	0.2520	1.0000	0.3269	-0.2481	0.1145
if	-0.1578	0.5181	0.4884	0.3269	1.0000	-0.5839	-0.1579
iw	0.4979	-0.6731	-0.1192	-0.2481	-0.5839	1.0000	0.4989
a	1.0000	-0.3206	0.4151	0.1145	-0.1579	0.4989	1.0000

Figure 24 Correlation coefficients for Step B

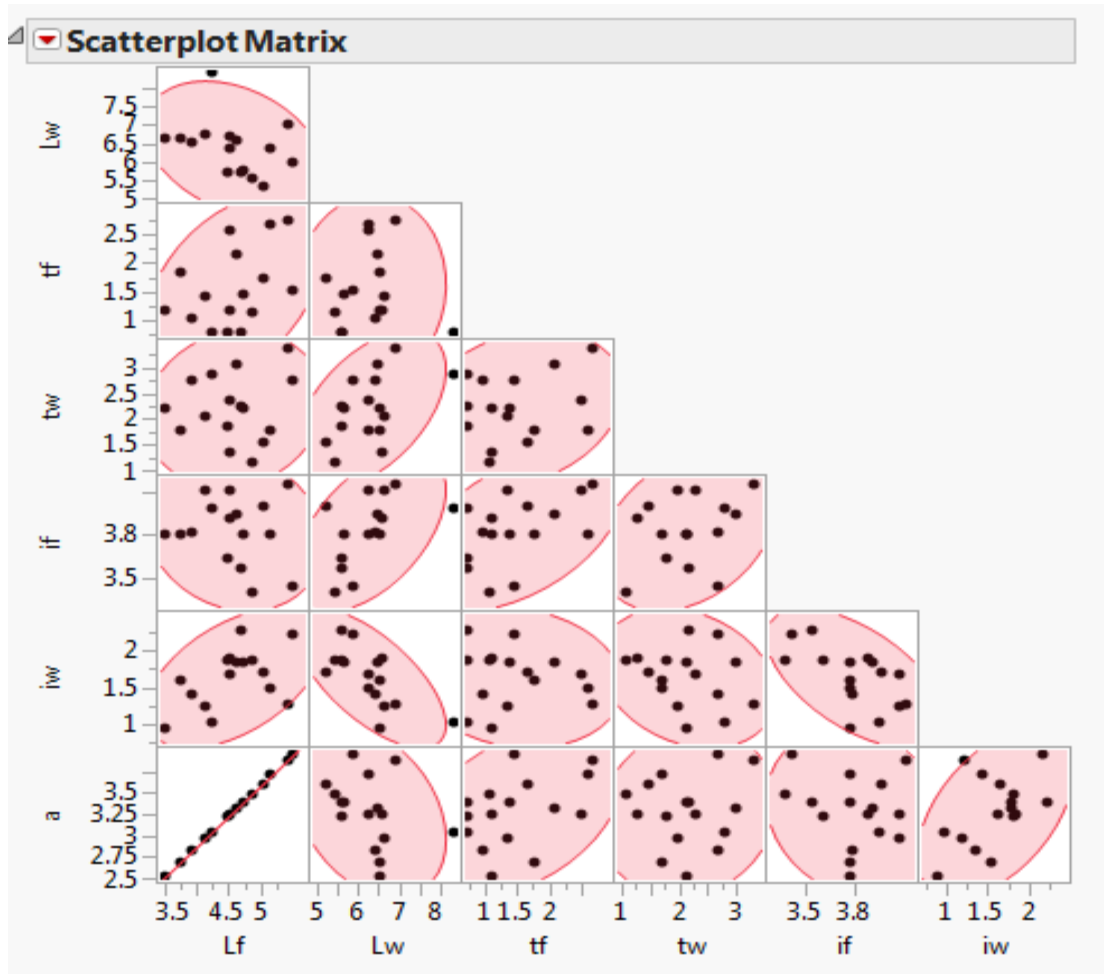


Figure 25 Bivariate relationships between response parameters for Step B

The same graph was plotted for the welding data obtained from Step C and it is shown in Figure 26. The correlation matrix for Step C is presented in Figure 27. The main results of this correlation analysis for Step C are summarized below:

- 1) Low positive correlation
  - tf and Lf
  - iw and Lf
  - a and tf
- 2) Low negative correlation
  - Lw and Lf
  - if and iw
- 3) Moderate positive correlation
  - tw and Lw
- 4) Perfect positive correlation
  - Lf and a

As it is evident, in both scatterplot matrices for Steps B and C, there is a perfect and strong positive correlation respectively between bead thickness (a) and Lf, as bead thickness is derived from the leg lengths, and especially from the shorter length (most often Lf). The process of bead thickness calculation is presented in Chapter 3.

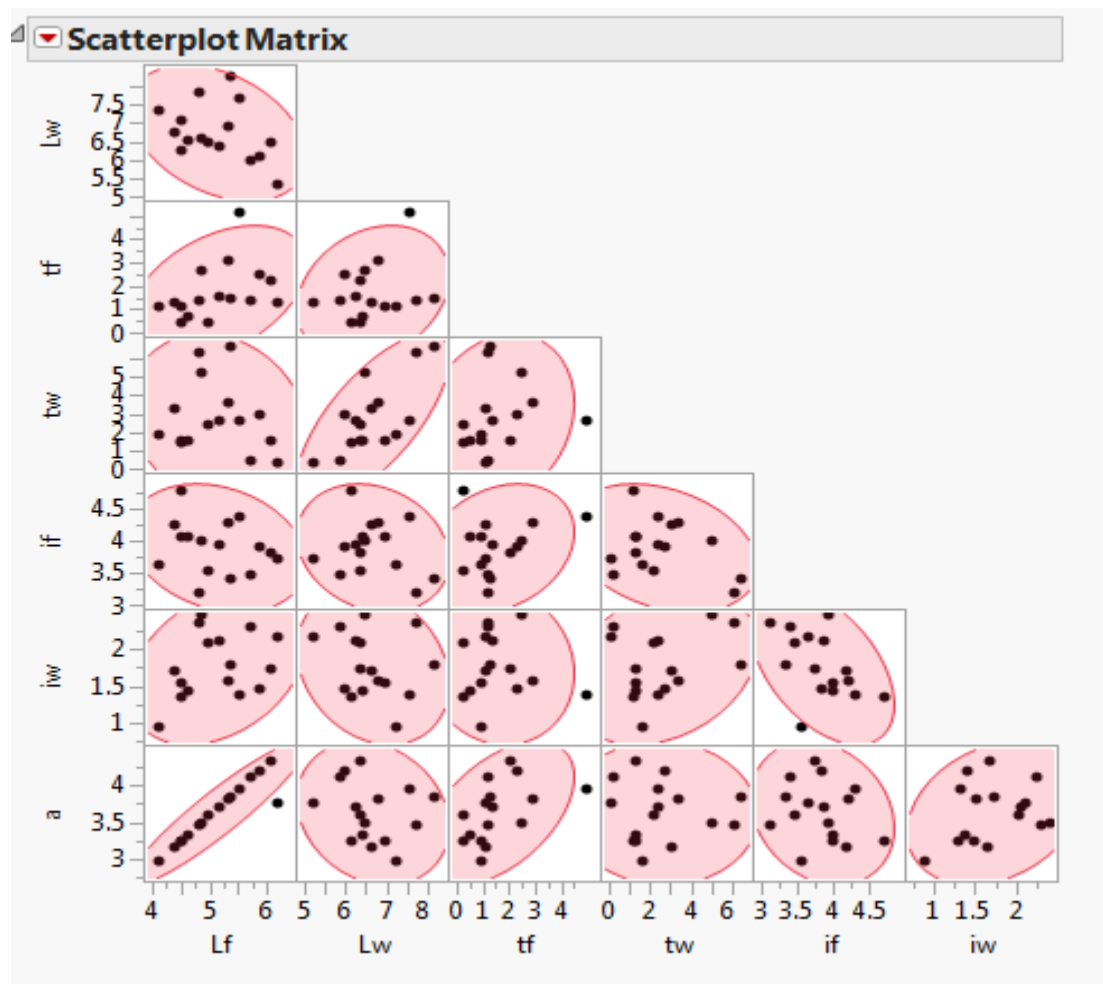


Figure 26 Bivariate relationships between response parameters for Step C

Multivariate							
Correlations							
	Lf	Lw	tf	tw	if	iw	a
Lf	1.0000	-0.3639	0.4187	-0.1593	-0.2385	0.3333	0.9260
Lw	-0.3639	1.0000	0.2435	0.7078	-0.1918	-0.2244	-0.1942
tf	0.4187	0.2435	1.0000	0.1910	0.2499	-0.0860	0.5068
tw	-0.1593	0.7078	0.1910	1.0000	-0.2996	0.2797	-0.0336
if	-0.2385	-0.1918	0.2499	-0.2996	1.0000	-0.4900	-0.2108
iw	0.3333	-0.2244	-0.0860	0.2797	-0.4900	1.0000	0.2699
a	0.9260	-0.1942	0.5068	-0.0336	-0.2108	0.2699	1.0000

Figure 27 Correlation coefficients for Step C

Another part of bivariate relationships' investigation consists of analyzing the two welding data sets from Steps B and C together. The scatterplots, which are shown in Figure 29, reveal the nature of the relationship among input and output parameters. The correlation analysis (Figure 28) can be summarized in the following findings:

- 1) Low positive correlation
  - a and WF
  - iw and X
  - iw and welding position
  - a and welding position
  - if and tf
  - a and tf
  - a and iw
- 2) Low negative correlation
  - tf and X
  - if and X
  - tf and Y
  - tf and welding position
  - tw and welding position
  - iw and if
- 3) Moderate negative correlation
  - a and Y

Multivariate									
Correlations									
	Wire Feed	Angle X	Angle Y	Welding Position	tf	tw	if	iw	a
Wire Feed	1,0000	-0,0000	0,0000	-0,0000	0,1001	0,1992	0,1025	0,1708	0,4166
Angle X	-0,0000	1,0000	-0,0000	-0,0000	-0,3269	0,1875	-0,5531	0,4079	-0,1519
Angle Y	0,0000	-0,0000	1,0000	0,0000	-0,5145	-0,1815	0,0434	-0,0467	-0,6354
Welding Position	-0,0000	-0,0000	0,0000	1,0000	-0,3028	-0,5260	-0,2089	0,3955	0,4207
tf	0,1001	-0,3269	-0,5145	-0,3028	1,0000	0,2118	0,3147	-0,0761	0,4538
tw	0,1992	0,1875	-0,1815	-0,5260	0,2118	1,0000	-0,1726	0,1749	0,0866
if	0,1025	-0,5531	0,0434	-0,2089	0,3147	-0,1726	1,0000	-0,4812	-0,1255
iw	0,1708	0,4079	-0,0467	0,3955	-0,0761	0,1749	-0,4812	1,0000	0,4083
a	0,4166	-0,1519	-0,6354	0,4207	0,4538	0,0866	-0,1255	0,4083	1,0000

Figure 28 Correlation coefficients for input and output parameters and for both Steps B & C

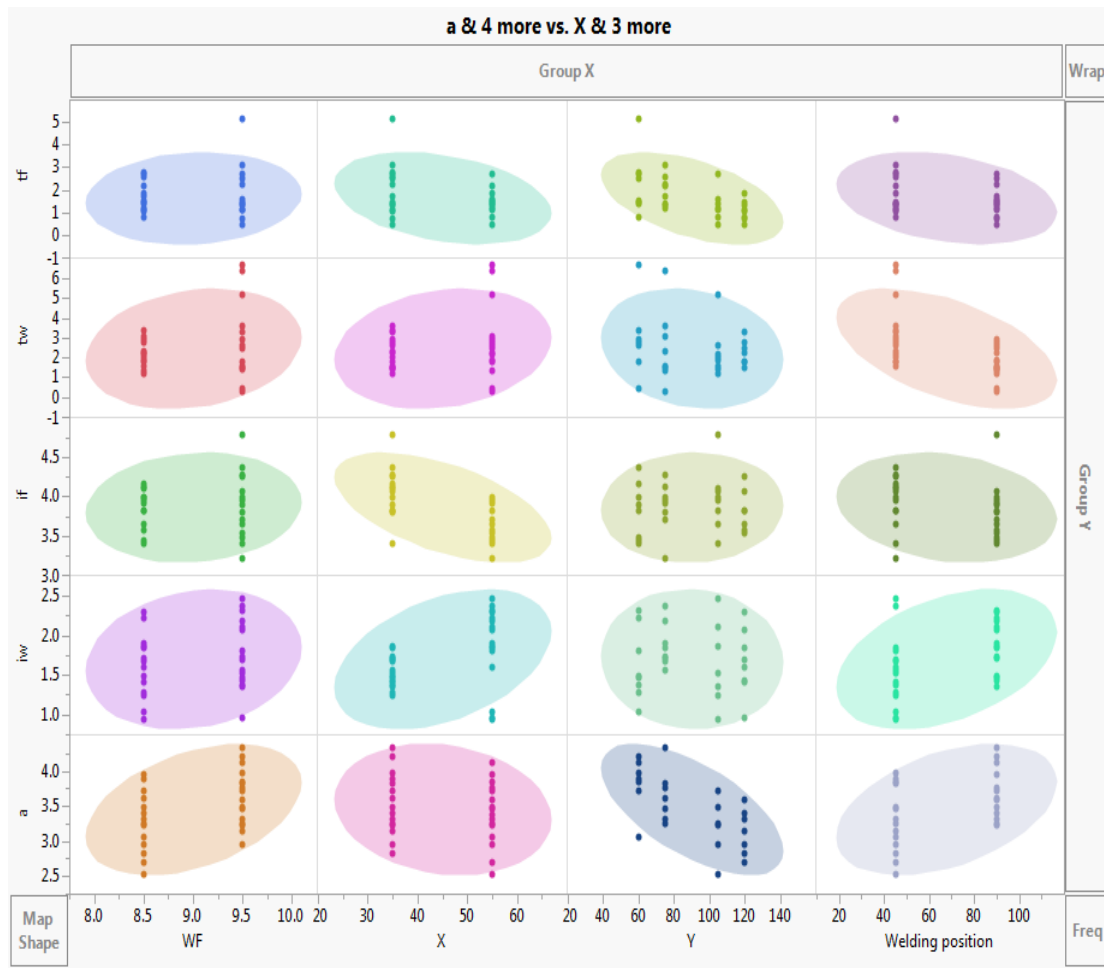


Figure 29 Bivariate relationships between response and input parameters for Steps B & C together

#### 4.2.4 Prediction models

In order to further study the effect of control parameters on the final weld geometry and weld dimensions, prediction models were constructed for each response variable with JMP11 software. The derived equations are built using standard least square regression and can predict the values of penetration, toe radius and bead thickness in terms of the wire feed, gun angles and welding position. Interaction effects among the input variables were also taken into consideration. The prediction expression of all response variables are presented below:

- $tf = 4.0249 - 0.0203*(Y) - 0.0306*(X) - 0.0126*(\text{Welding position}) + 0.1875*(WF) + (Y-90)[(X-45)*0.0017]$
- $tw = -0.5325 - 0.0327*(\text{Welding position}) + 0.5569*(WF) + 0.0262*(X) - 0.0107*(Y) + (\text{Welding position}-67.5)*[(WF-9)*(-0.0346)] + (\text{Welding position}-67.5)*[(X-45)*(-0.0012)]$

- $if = 4.2255 - 0.0179*(X) - 0.003*(\text{Welding position}) + 0.0663*(WF) + 0.0006*(Y) + (X-45)*[(WF-9)*9-0.022] + (WF-9)*[(Y-90)*0.0072]$
- $iw = -0.6958 + 0.0166*(X) + 0.0071*(\text{Welding position}) + 0.1388*(WF) - 0.008*(Y) + (X-45)*[(\text{Welding position}-67.5)*0.0003] + (X-45)*[(WF-9)*0.0184] + (\text{Welding position}-67.5)*[(WF-9)*(-0.0091)]$
- $a = 1.0389 + 0.3562*(WF) - 0.0066*(X) - 0.0114*(Y) + 0.008*(\text{Welding position})$

The value of the  $R^2$  for the models was above 0.50. Moreover, the residual plots, which were also built for each response variable, did not reveal any pattern, therefore the prediction models can be perceived valid and accurate.

As it is obvious from the above equations, both main and interaction effects between the input variables have been taken into account in order to construct the models. These interactions are presented graphically in Figures 30-33.

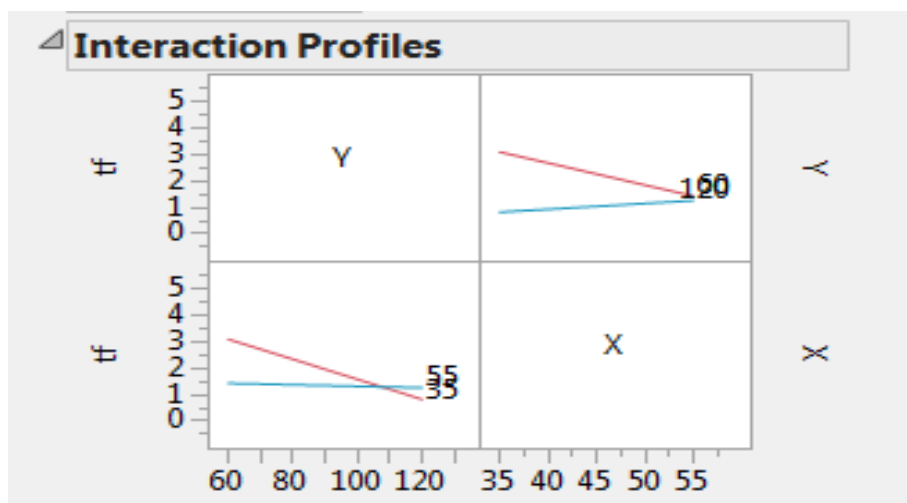


Figure 20 Interactions for tf

As we notice in Figure 30, while welding at an X angle of 35 degrees and when we go from “push” to “pull”, the toe radius in the flange plate decreases. In contrast, the toe radius remains almost constant when welding with a gun angle X of 55 degrees.



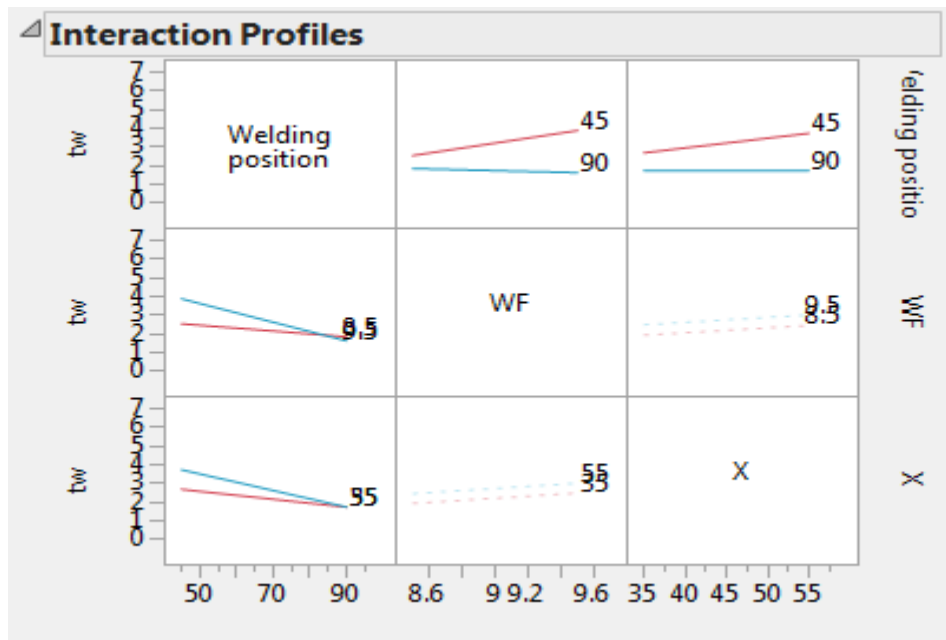


Figure 31 Interactions for *tw*

Concerning *tw*, as we notice in Figure 31, when welding at PA position (45 degrees) and while increasing the wire feed rate, toe radius in the waist plate increases. The same result is observed for *tf* when the gun angle *X* is increasing from 35 to 55 degrees. In contrast, PB position is related with more stable results for *tw*.

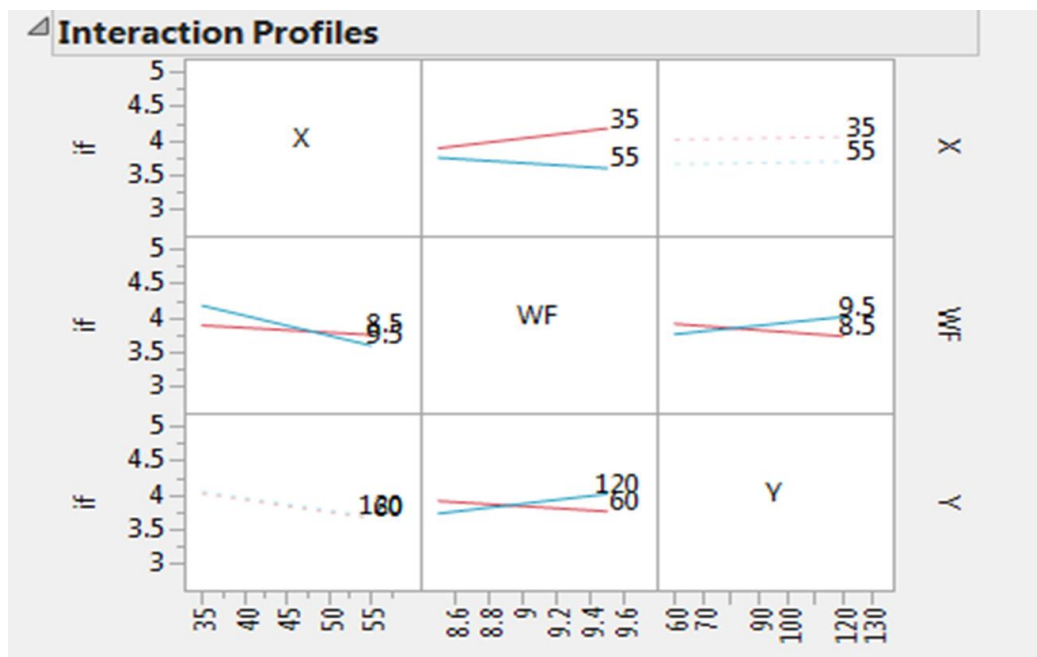


Figure 32 Interactions for *if*

Moreover, as it is observed in Figure 32, while welding with an angle of 35 degrees, penetration in the flange plate increases with wire feed rate. The opposite result is observed for the angle of 55 degrees, which is related with a drop in the penetration when wire feed rate increases. Additionally, it is noticed that in the “push” direction, penetration in the flange plate increases

with the wire feed rate. In contrast, penetration drops when wire feed rate increases when welding in the “pull” direction.

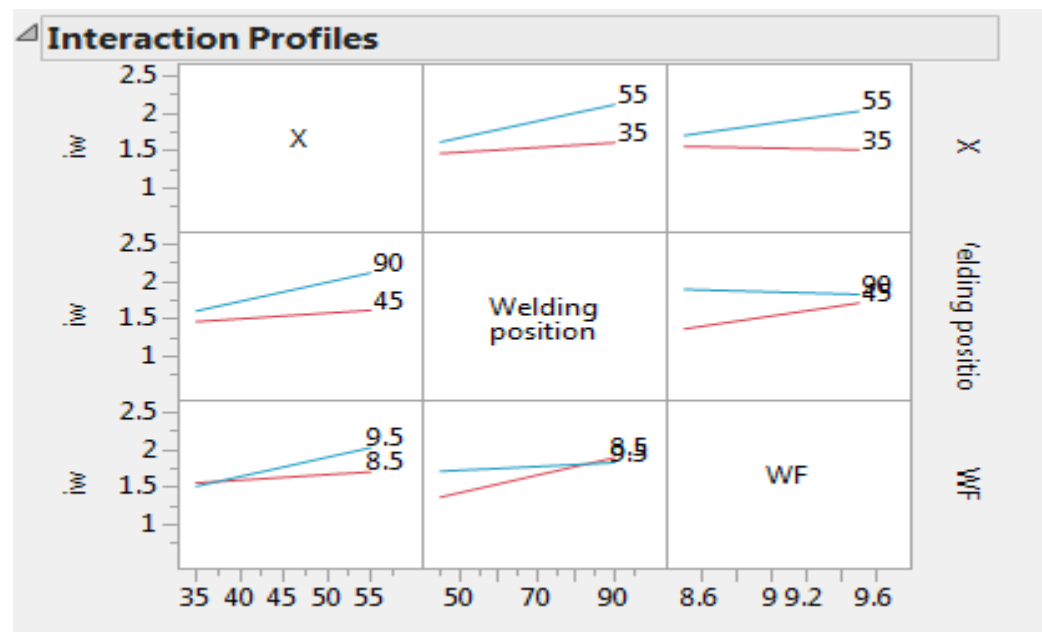


Figure 33 Interactions for iw

Regarding interactions for iw, it can be pointed out from Figure 33 that while welding at a gun angle X of 55 degrees, penetration in the waist plate increases with wire feed rate.

Summarizing the observations regarding penetration in both plates, it can be concluded that penetration in the flange plate can be maximized with a gun angle X of 35 degrees. In contrast, penetration in the waist plate is more easily maximized at an angle X of 55 degrees.

#### 4.3 Step D

In step D of the experiments, some selected tests were repeated in four different travelling speeds, as explained in the previous chapter. A correlation analysis of the obtained data was performed in order to investigate the influence of higher travelling speeds and angle Y on response parameters. The results of this analysis are presented in Figure 34.

Multivariate									
Correlations									
	Angle Y	Tr. Speed	Lf	Lw	tf	tw	if	iw	a
Angle Y	1.0000	-0.0000	-0.1719	-0.7939	-0.2528	-0.6960	-0.1741	0.7019	-0.1719
Tr. Speed	-0.0000	1.0000	-0.5418	-0.3835	0.1374	0.2539	-0.1650	-0.1085	-0.5418
Lf	-0.1719	-0.5418	1.0000	0.2848	0.3102	-0.0673	-0.4693	0.1529	1.0000
Lw	-0.7939	-0.3835	0.2848	1.0000	0.0429	0.6560	0.2561	-0.5449	0.2848
tf	-0.2528	0.1374	0.3102	0.0429	1.0000	0.0605	-0.2547	-0.1038	0.3102
tw	-0.6960	0.2539	-0.0673	0.6560	0.0605	1.0000	0.1598	-0.4130	-0.0673
if	-0.1741	-0.1650	-0.4693	0.2561	-0.2547	0.1598	1.0000	-0.5338	-0.4693
iw	0.7019	-0.1085	0.1529	-0.5449	-0.1038	-0.4130	-0.5338	1.0000	0.1529
a	-0.1719	-0.5418	1.0000	0.2848	0.3102	-0.0673	-0.4693	0.1529	1.0000

Figure 34 Correlation coefficients for Step D

As it can be remarked, there is a moderate negative correlation between angle Y and Lw, as well as between angle Y and tw. Moreover, there is a moderate positive correlation between angle Y and iw. Regarding travelling speed, there is a low negative correlation between travelling speed and Lf, Lw and bead thickness (a) respectively. The results are shown graphically in Figure 35.

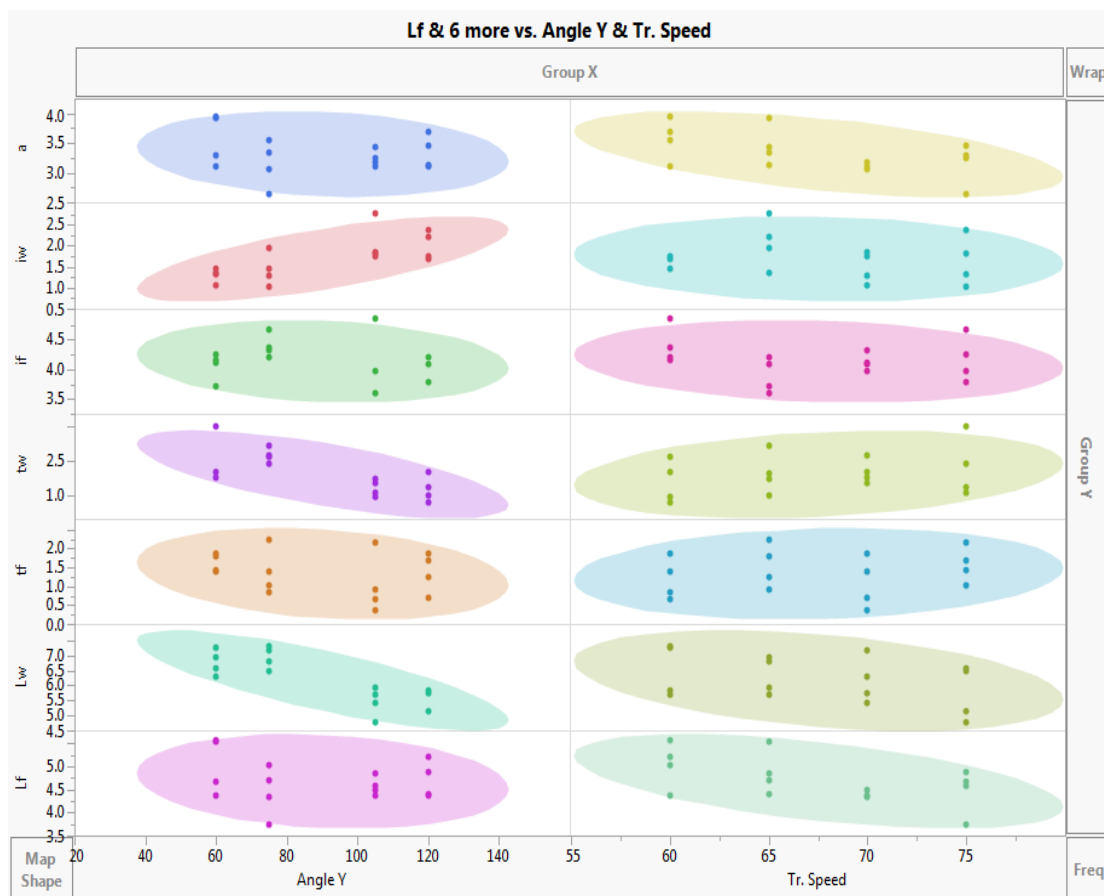


Figure 35 Bivariate relationships between response and input parameters for Step D

Additionally, in order to investigate which settings produce the most favorable welds, which are not defective, the distribution of data obtained in Step D were plotted in JMP11 software, as it is shown in Figure 36.

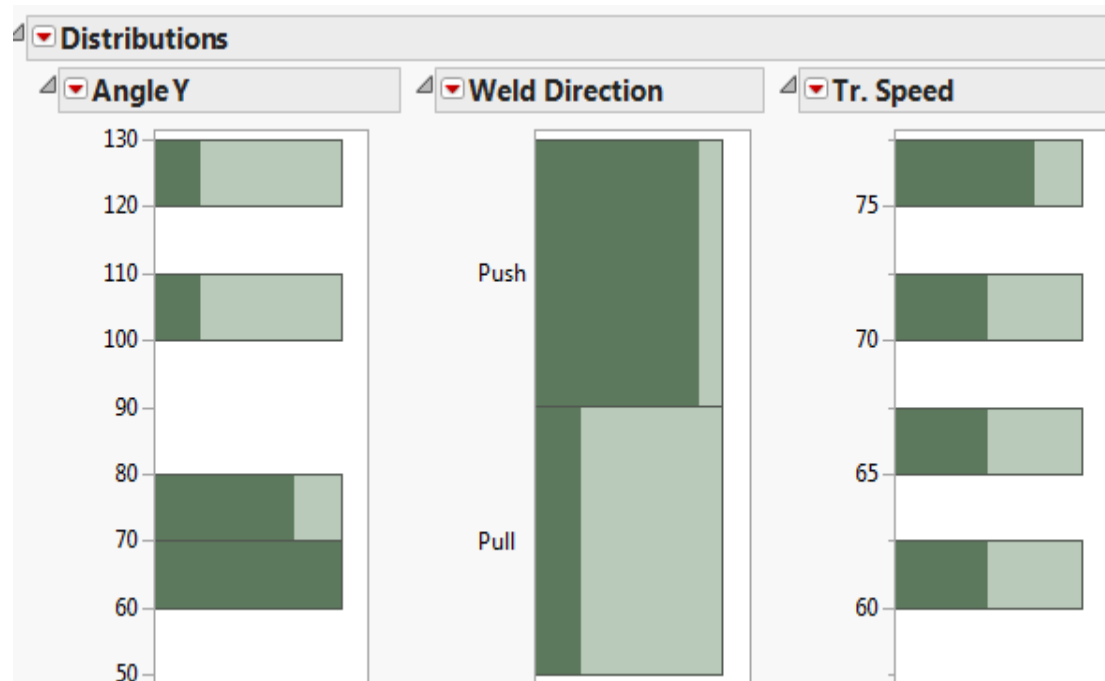


Figure 36 Distribution of input variable for Step D. The dark green area corresponds to the welds that fulfill all requirements

In the graph presented above, it can be observed that a combination of welding in the "push" direction with a travelling speed of 75cm/min produces the most favorable welds.

#### 4.4 Step E – Pulsed welding

Concerning Step E several test runs were reproduced using pulsed welding as explained in the previous chapter.

A distribution plot was created for step E in order to observe which of the weld specimens fulfill geometry limitations, which were set previously.

Dark green areas in Figures 37 and 38 depict which input and output parameters correspond to requirements. From all 12 weld tests 4 were accepted and especially those with low wire feed rate and travelling speeds. Moreover, push direction and PA position appeared to be the most favorable settings for pulsed welding.

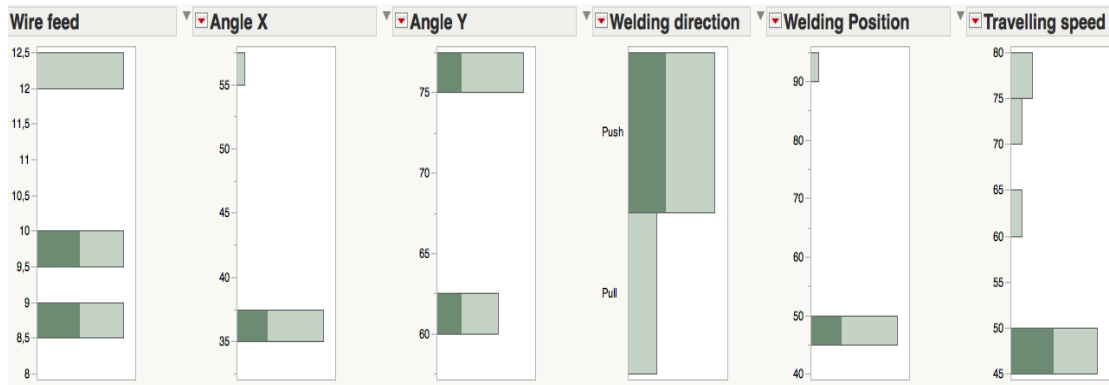


Figure 37 Distribution for pulsed welding - input parameters (Step E)



Figure 38 Distribution for pulsed welding - output parameters (Step E)

From Figure 38 it was noticed that among all test runs only those with low values of penetration and toe waist fulfilled all requirements.

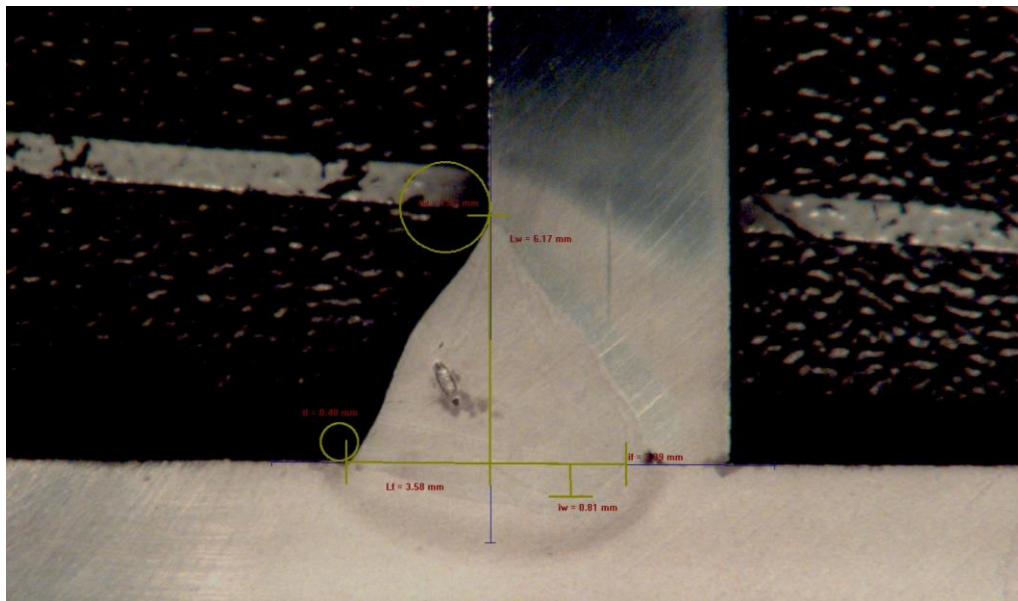


Figure 39 Test sample from pulsed welding showing porosity

Moreover, it was observed that pulling the welding gun produced defective or unaccepted welds in general, as shown in Figure 39.

Charts of penetration and bead thickness were created for all test runs.

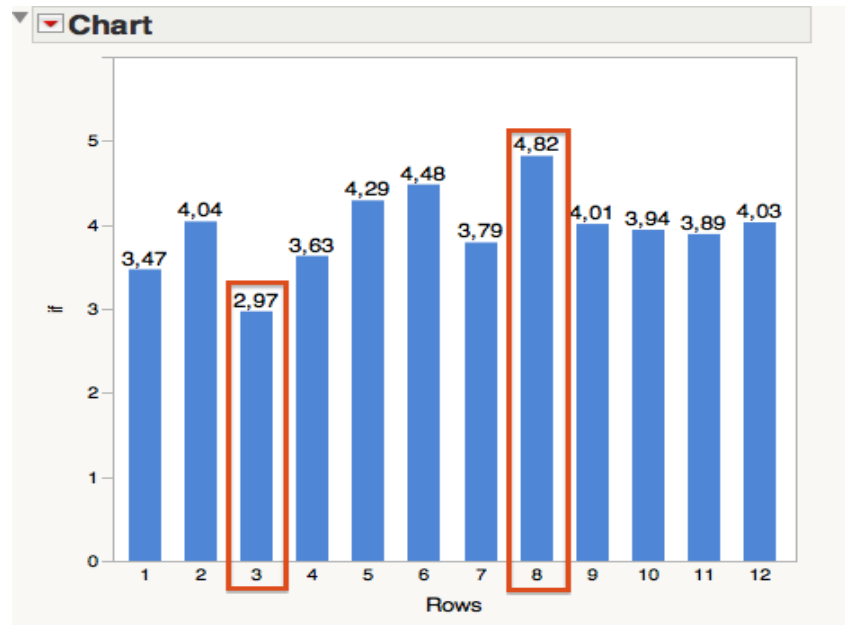


Figure 40 Penetration chart for Step E where lowest and highest values are marked

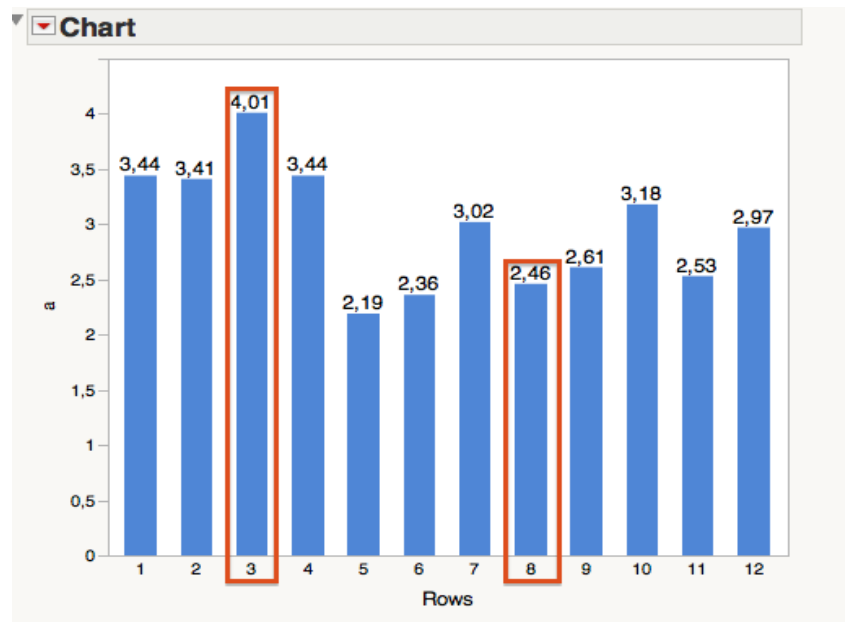


Figure 41 Bead thickness chart for Step E where lowest and highest values are marked

It is evident from Figures 40 and 41 that when a sample shows high penetration then its bead thickness is low and vice versa.

Taking under consideration the findings from previous figures, correlation charts between all geometry responses were plotted. A scatterplot between all output parameters and their R coefficients are seen in Figures 42 and 43.

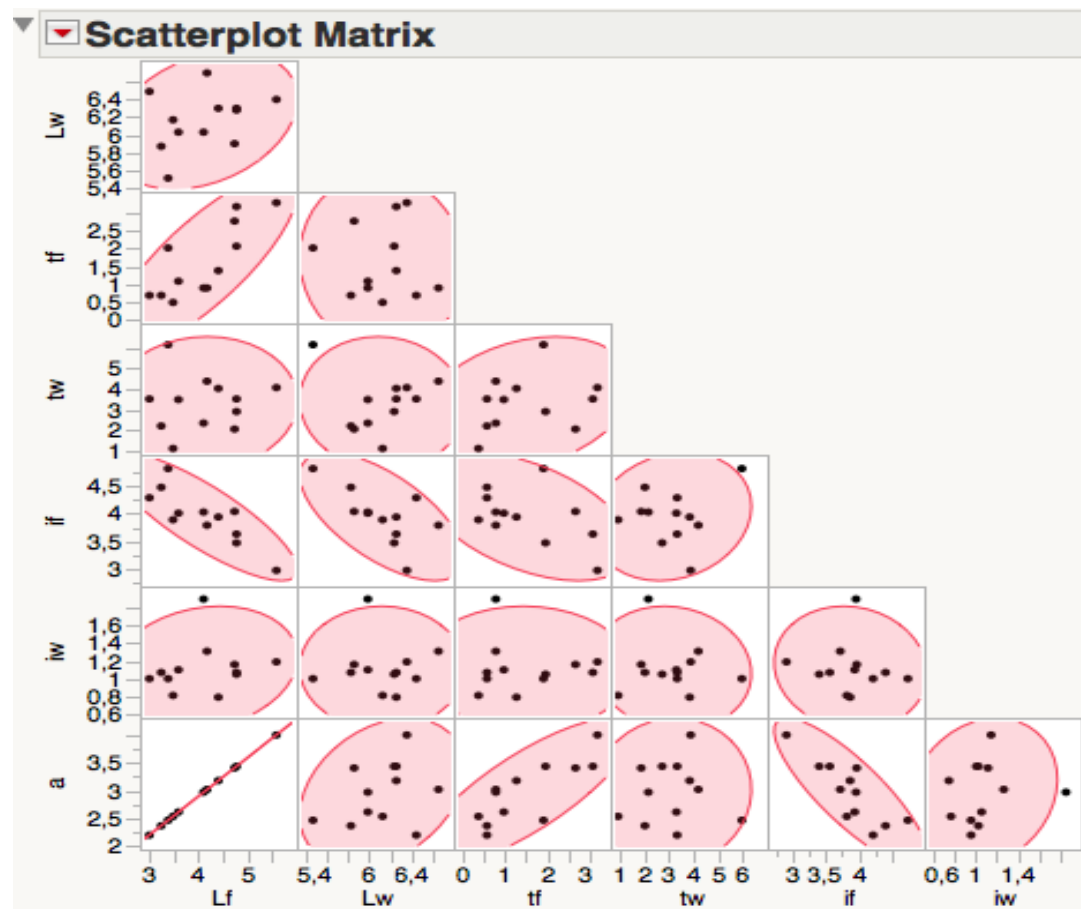


Figure 42 Scatterplot matrix showing all bivariate relationships between response parameters for Step E

Multivariate							
Correlations							
	Lf	Lw	tf	tw	if	iw	a
Lf	1,0000	0,3141	0,7969	0,0387	-0,8306	0,1743	1,0000
Lw	0,3141	1,0000	-0,0548	-0,0457	-0,6430	-0,0016	0,3147
tf	0,7969	-0,0548	1,0000	0,2768	-0,4922	-0,0309	0,7959
tw	0,0387	-0,0457	0,2768	1,0000	0,1615	-0,0964	0,0394
if	-0,8306	-0,6430	-0,4922	0,1615	1,0000	-0,0899	-0,8308
iw	0,1743	-0,0016	-0,0309	-0,0964	-0,0899	1,0000	0,1756
a	1,0000	0,3147	0,7959	0,0394	-0,8308	0,1756	1,0000

Figure 43 R coefficients for pulsed welding. Strongest correlation values are marked

Alike with previous steps and using the same ranking correlations among variables, results for Step E can be summarized into the following points

- 1) Low positive correlation
  - Lw and Lf

- a and Lw
- 2) Low negative correlation
  - if and tf
- 3) Negative moderate correlation
  - if and Lw
- 4) Strong positive correlations
  - tf and Lf
  - tf and a
- 5) Strong negative correlations
  - if and Lf
  - if and a
- 6) Perfect positive correlation
  - Lf and a

Perfect positive correlation between Lf and bead thickness is expected as explained in previous steps.

Furthermore, a comparison between response parameters of pulsed and conventional welding was created for those test runs, which satisfied response limitations (Figure 44).

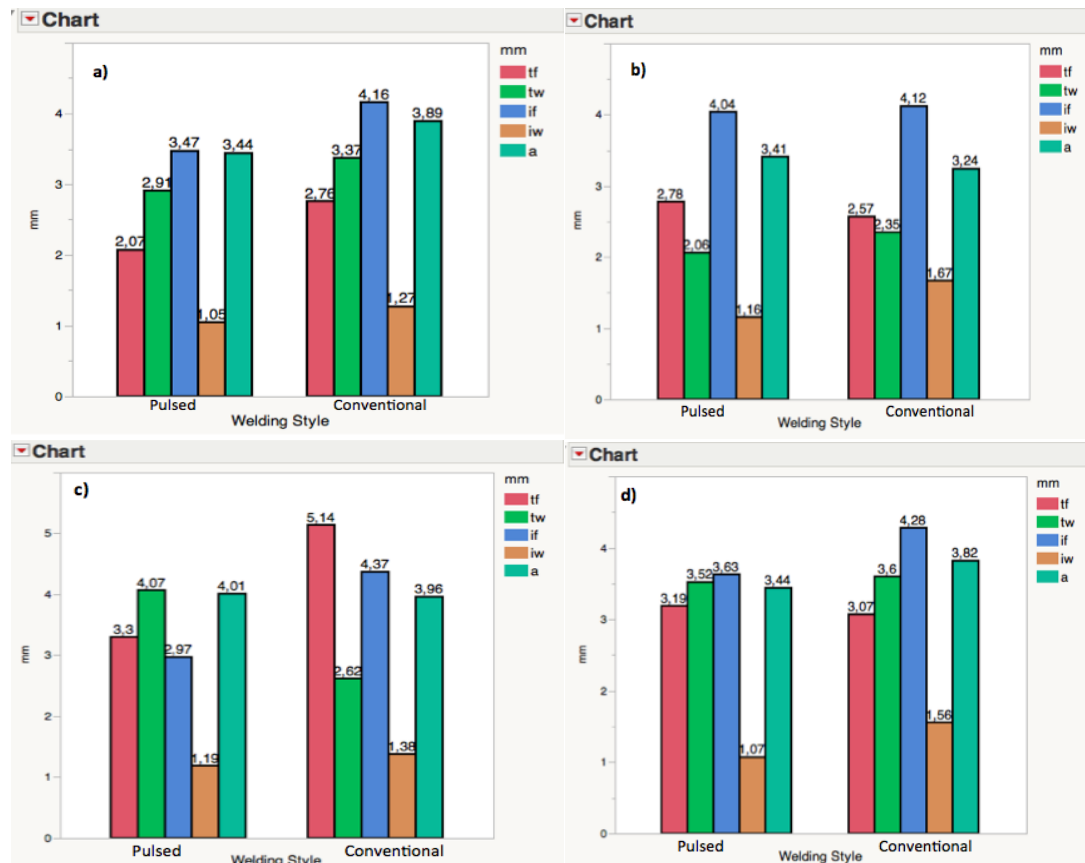


Figure 44 Comparison charts of response values for test runs a) MC 37, b) MC38, c) MC39, d) MC40 (Appendix A)

In general Figure 44 reveals higher values of bead thickness (a) and penetration (if, iw) when it comes for conventional welding.



## 5. Discussion

Considering Step A, the three welds performed, showed a 30% higher penetration in flange plate and a 35% smaller bead thickness in comparison to the previous identical tests conducted by Hammersberg & Olsson (2013). This can be explained by the existence of a prepared edge on the waist plates during welding in Step A. This small groove can allow more filler material to penetrate by hindering the creation of large bead.

Regarding the analysis of the experiments from Steps B and C, a point which should be remarked is that even though welding with higher wire feed rate produced higher mean values in the response variables, it was accompanied by more variation. In contrast, welding with the lower wire feed rate of 8.5m/min was a more stable process. This result opens a discussion on how the multiparameter problem of optimizing GMAW should be treated. The approach of this problem should firstly clarify whether robustness (no variation) or specific target values for the responses is the desired goal.

Another finding from the same series of experiments was that the combination of “Push” welding direction, 35 degrees of X gun angle and PA position produced the welds with the higher quality according to the specification limits which were set for response variables. This optimal combination of settings applies for both wire feed rates (8.5 and 9.5 m/min) in Steps B and C maximizes penetration, toe radius and bead thickness.

Moreover, the analysis performed in JMP11 revealed correlations between the response variables for Steps B and C. In general, regarding both Steps B and C, a positive correlation between toe radius and leg length in each plate is observed. This result is expected, as, when the leg length in the flange plate increases for instance, the angle between the weld bead and the plate increases. Therefore, a bigger adjacent circle to the flange plate can be drawn, which means larger toe radius (Figure 17).

Another observation from the analysis was that bead thickness increases when toe radius in the flange plate increases. This result is logical since both those two parameters are proportionally related to the leg length of the flange plate,  $L_f$ . In addition, it was found that the leg length of the waist plate decreases, as penetration in the waist plate increases. This is happening because bigger amount of filler material concentrated in the bottom of the weld ( $i_w$ ), means less material in the upper part of the weld ( $L_w$ ). In the same way the negative correlation between penetration in the flange and penetration in the waist plate can be explained. In other words, the more filler material penetrates horizontally (if), the less penetrates vertically ( $i_w$ ).

Regarding correlation between input and output variables in Steps B and C, it was found that in position PA, larger toe radii can be achieve. This can be related to the fact that the force of gravity on the filler material results in a more uniform bead. In other words, the filler material solidifies into a more symmetrical geometry in PA than in PB, and therefore a smoother curve is formed in the transition from the weld bead to both plates (Figure 16). As a

result, larger adjacent circles to the plates and bigger toe radii are expected in PA.

In contrast, PB welding position is related with higher bead thickness, regarding Steps B and C. This is due to the fact that in PB position the force of gravity drags the filler material towards the flange plate, increasing  $L_f$ , and therefore the bead thickness.

Another result from the analysis in Steps B and C was that welding in the “pull” direction, results in smaller bead thickness. This is an expected result, because as presented in Chapter 2, pushing the weld gun creates shallower and wider weld geometry, while pulling creates a deeper and narrower profile.

Regarding the series of experiments from Step D, it is highly notable that the combination of “push” and the highest travelling speed (75cm/min) produced the welds with the higher quality. Therefore a 56% increase in the productivity can be achieved in comparison to Steps A, B and C.

Moreover it is observed that welding in the “pull” welding direction in Step D, produces many defective welds with lower toe radius and leg length in the waist plate. In contrast, penetration in the waist plate increased with welding in the “Pull” direction. In addition, a negative correlation is noticed between travelling speed and bead thickness is noticed in general. This result is due to the fact that less filler material per minute is deposited on the area of the weld when travelling speed is increased.

As far as pulsed welding is concerned, distribution charts revealed that high travelling speeds and wire feed rates couldn't fulfill weld geometry requirements. This can be interpreted as an inability of pulsed welding to enhance productivity. However, it should be mentioned that voltage in this series of experiments was relatively low compared to previous steps; therefore, further research on the impact of voltage needs to be carried. As in previous steps, settings in push direction and angle  $X 35^\circ$  were the most favorable settings. On the same time pulling the gun produced defective or unaccepted welds. Therefore, in combination with the previous findings it is evident that pull direction is ineffective.

Bivariate relationships as shown in the scatterplot matrix revealed stronger correlations between bead thickness (a), penetration flange (if) and toe radius in flange (tf) than in previous Steps. These strong correlations explain the results in distribution charts and clearly state that in pulsed welding only a trade-off between values of bead thickness and penetration can create a quality weld.

In general, it can be said that in pulsed welding, since correlations between response parameters are strong, optimized settings can be created with more accuracy for a desired weld.

Comparisons show that bead thickness and penetration in pulsed welding have lower values than conventional style of welding. This result can be

explained by the strong correlations between response parameters as mentioned previously and by the low value of voltage that was used in this series. Therefore, this loss can be compensated by providing higher voltage.



## 6. Conclusions

Five different series of experiments in robotized Gas Metal Arc Welding of mild steel plates in a Tee joint geometry were performed. The main purpose has been to investigate the influence of process input parameters on weld quality when using metal cored wires. The specimens were cross sectioned, grinded and etched before they were measured. The measurement was performed through Lumenera software and the response parameters which were measured were penetration, toe radius, bead thickness and leg length. Specification limits were set for the response variables and statistical analysis was carried out through JMP11 software. The statistical analysis of the measurements was mainly focused on revealing the bivariate relationships, optimizing weld dimensions and developing prediction models of the responses in term of the input variables.

The five different series of experiments were performed in different Steps:

- Step A (solid wires): In order to verify results from previous research done in cooperation with VCE, 3 experiments with solid wire were repeated with the same settings
- Step B: 16 experiments with a wire feed speed of 8.5 m/min were performed by varying gun angles and welding position
- Step C: 16 experiments with a wire feed speed of 9.5 m/min were performed by varying gun angles and welding position
- Step D: 4 selected experiments from the previous steps were repeated at four different higher travelling speeds and a higher wire feed speed
- Step E: 12 selected experiments from all the previous steps were repeated in pulsed welding

The main conclusions for each Step were:

### Step A

- There is consistency between GMAW robots of VCE – Arvika and Elga AB

### Step B & C

- Push direction with angle X at 35° and PA position are the optimized settings according to the specifications which were set. Higher mean values for response variables but higher variation is observed when increasing the wire feed speed.

### Step D

- Higher productivity can be obtained when welding in push direction by increasing travelling speed.

### Step E

- Strong correlations between geometry output responses. Only a trade-off between values of bead thickness and penetration can create a

quality weld. Less total amount of high quality welds are observed, in comparison with conventional welding.

## References

- Davis, A., 2009, Optimizing Metal Cored Performance, *Penton's Welding Magazine*, 82(2), p. 12.
- Hammersberg, P. & Olsson, H., 2013, *Proactive control of weld dimensions in robotised MAG welding*.
- Ibrahim, I.A., Mohamat, S.A., Amir, A. & Ghalib, A., 2012, The Effect of Gas Metal Arc Welding (GMAW) Processes on Different Welding Parameters, *Procedia Engineering*, 41, pp. 1502-6.
- Iordachescu, D. & Quintino, L., 2008, Steps toward a new classification of metal transfer in gas metal arc welding, *Journal of Materials Processing Technology*, 202(1–3), pp. 391 - 397.
- Jackson, S. *Research Methods and Statistics: A Critical Thinking Approach*. Cengage Learning, 2008.
- Karadeniz, E., Ozsarac, U. & Yildiz, C., 2007, The effect of process parameters on penetration in gas metal arc welding processes, *Materials & Design*, 28(2), pp. 649-56.
- Kuvin, B.F., 1998, Metal-cored wire outwelds flux cored, *Welding Design & Fabrication, Including Welding Engineer*, 71(10), p. 12.
- Liao, M.T. & Chen, W.J., 1999, A Comparison of Gas Metal Arc Welding with Flux-Cored Wires and Solid Wires Using Shielding Gas, *International Journal of Advanced Manufacturing Technology*, 15(1), pp. 49-53.
- O'Brien, R.L., 1991, *Welding handbook: Vol. 2, Welding processes*, American Welding Society, Miami, Fla.
- Palani, P.K. & Murugan, N., 2006, Selection of parameters of pulsed current gas metal arc welding, *Journal of Materials Processing Tech*, 172(1), pp. 1-10.
- Praveen, P., Yarlagadda, P. & Kang, J., 2005, Advancements in pulse gas metal arc welding, *Journal of Materials Processing Technology*, 164-165, pp. 1113-9.
- Ramos-Jaime, D., Juárez, I.L. & Perez, P., 2013, Effect of Process Parameters on Robotic {GMAW} Bead Area Estimation, *Procedia Technology*, 7(0), pp. 398 - 405.
- Ryan, Thomas P. *Statistical Methods for Quality Improvement*. New York: Wiley, 2000.

Weman, K., 2011, *Welding Processes Handbook*, Woodhead Publishing, Burlington.

Weman, K., Lindén, G., collection), B.-E., Books24x7, I. & Institute of Materials (London, E., 2006, *MIG welding guide*, Woodhead Publishing,.



## Appendix A – Experiments

Step	Test name	Input Parameters									Output Parameters								Defects
		Voltage (V)	Wf (m/min)	Amperage (A)	Stick Out (mm)	Angle X	Angle Y	Weld Direction	Weld position	Tr. Speed (cm/min)	Lf	Lw	tf	tw	if	iw	a	a calculation	
Step A	S1 (slit=1.5)	29,5	15	355	20	45	90	-	90	48	4,83	6,37	0,68	1,2	6,78	4,1	3,42	3,415325753	Porosity
	S2	29,5	15	340	20	55	75	Push	90	48	5,7	7,23	0,36	1,47	4,47	2,67	4,04	4,030508653	
	S3	29,5	15	345	20	55	75	Push	90	48	5,82	6,99	0,72	1,39	3,77	3,13	4,12	4,115361467	
*	Test 1	29,5	15	350	20	45	90	-	90	48	-	-	0,85	4,2	5,39	4,66	4,93	-	
*	Test 2	29,5	15	350	20	55	75	push	90	48	-	-	0,5	4,7	3,47	3,17	5,5	-	
*	Test 3	29,5	15	350	20	55	75	push	90	48	-	-	1	2,75	3,1	2,98	5,42	-	
Step B & C	MC1	28,7	8,5	245	20	35	60	Push	90	48	5,24	6,39	2,68	1,79	3,81	1,49	3,71	3,705239533	
	MC2	28,7	8,5	245	20	35	75	Push	90	48	5,1	5,31	1,72	1,56	4	1,72	3,61	3,606244584	
	MC3	28,7	8,5	245	20	55	60	Push	90	48	5,58	6	1,51	2,75	3,44	2,23	3,95	3,945655839	
	MC4	28,7	8,5	250	20	55	75	Push	90	48	4,59	6,7	1,16	1,35	3,92	1,91	3,25	3,245620126	Undercut
	MC5	28,7	8,5	250	20	35	120	Pull	90	48	4,79	5,76	1,47	2,22	3,81	1,84	3,39	3,387041482	
	MC6	28,7	8,5	250	20	35	105	Pull	90	48	4,93	5,53	1,12	1,17	3,4	1,87	3,49	3,486036431	
	MC7	28,7	8,5	245	20	55	120	Pull	90	48	4,78	5,72	0,79	2,24	3,57	2,29	3,38	3,379970414	
	MC8	28,7	8,5	247	20	55	105	Pull	90	48	4,55	5,69	0,77	1,85	3,64	1,87	3,22	3,217335854	
	MC9	29,8	9,5	265	20	55	120	Pull	90	48	5,07	6,5	0,47	2,45	3,54	2,08	3,59	3,585031381	
	MC10	29,8	9,5	270	20	55	105	Pull	90	48	5,24	6,39	1,58	2,64	3,95	2,11	3,71	3,705239533	
	MC11	29,8	9,5	270	20	35	105	Pull	90	48	4,57	6,27	0,44	1,39	4,79	1,36	3,24	3,23147799	
	MC12	29,8	9,5	265	20	35	120	Pull	90	48	4,69	6,53	0,72	1,48	4,06	1,43	3,32	3,316330804	

	MC13	29,8	9,5	270	20	55	60	Push	90	48	5,81	5,97	1,37	0,47	3,47	2,32	4,11	4,10829039 9	
	MC14	29,8	9,5	270	20	55	75	Push	90	48	6,26	5,31	1,33	0,3	3,71	2,18	3,76	3,75473700 8	Undercut
	MC15	29,8	9,5	275	20	35	75	Push	90	48	6,13	6,5	2,26	1,52	3,8	1,74	4,34	4,33456456 9	
	MC16	29,8	9,5	270	20	35	60	Push	90	48	5,96	6,08	2,53	2,9	3,9	1,46	4,22	4,21435641 6	
	MC17	28,7	8,5	245	20	35	60	Push	45	48	5,5	7,04	2,76	3,37	4,16	1,27	3,89	3,88908729 7	
	MC18	28,7	8,5	245	20	35	75	Push	45	48	4,59	6,39	2,57	2,35	4,12	1,67	3,25	3,24562012 6	
	MC19	28,7	8,5	245	20	55	60	Push	45	48	4,31	8,47	0,79	2,89	3,99	1,03	3,05	3,04763022 7	
	MC20	28,7	8,5	250	20	55	75	Push	45	48	4,69	6,6	2,17	3,06	3,95	1,84	3,32	3,31633080 4	
	MC21	28,7	8,5	250	20	35	120	Pull	45	48	3,99	6,53	1,03	2,77	3,82	1,41	2,83	2,82135605 7	
	MC22	28,7	8,5	250	20	35	105	Pull	45	48	4,19	6,74	1,41	2,04	4,11	1,25	2,97	2,96277741 3	
	MC23	28,7	8,5	245	20	55	120	Pull	45	48	3,81	6,63	1,84	1,78	3,81	1,6	2,7	2,69407683 6	
	MC24	28,7	8,5	247	20	55	105	Pull	45	48	3,57	6,63	1,17	2,2	3,81	0,93	2,53	2,52437120 9	
	MC25	29,8	9,5	265	20	55	120	Pull	45	48	4,19	7,35	1,09	1,82	3,64	0,95	2,97	2,96277741 3	
	MC26	29,8	9,5	270	20	55	105	Pull	45	48	4,93	6,6	2,69	5,2	3,99	2,47	3,49	3,48603643 1	
	MC27	29,8	9,5	270	20	35	105	Pull	45	48	4,59	7,08	1,14	1,55	4,06	1,53	3,25	3,24562012 6	
	MC28	29,8	9,5	265	20	35	120	Pull	45	48	4,45	6,77	1,3	3,32	4,26	1,7	3,15	3,14662517 6	Porosity
	MC29	29,8	9,5	270	20	55	60	Push	45	48	5,45	8,3	1,46	6,68	3,4	1,8	3,86	3,85373195 7	
	MC30	29,8	9,5	270	20	55	75	Push	45	48	4,9	7,84	1,37	6,36	3,2	2,37	3,47	3,46482322 8	
	MC31	29,8	9,5	275	20	35	75	Push	45	48	5,41	6,94	3,07	3,6	4,28	1,56	3,83	3,82544768 6	
	MC32	29,8	9,5	270	20	35	60	Push	45	48	5,6	7,68	5,14	2,62	4,37	1,38	3,96	3,95979797 5	
	Step D																		
ref. MC27	MC33/1	31	12	320	20	35	105	Pull	45	60	4,38	5,72	0,66	0,95	4,85	1,76	3,1	3,09712770 2	
	MC33/2	31	12	320	20	35	105	Pull	45	65	4,86	5,94	0,91	1,72	3,6	2,77	3,44	3,43653895 7	Porosity
	MC33/3	31	12	320	20	35	105	Pull	45	70	4,49	5,4	0,36	1,56	3,97	1,86	3,18	3,17490944 8	
	MC33/4	31	12	320	20	35	105	Pull	45	75	4,59	4,76	2,17	1,14	3,97	1,83	3,25	3,24562012 6	
ref. MC21	MC34/1	31	12	320	20	35	120	Pull	45	60	5,22	5,84	1,86	0,73	4,21	1,7	3,7	3,69109739 8	
	MC34/2	31	12	320	20	35	120	Pull	45	65	4,4	5,72	1,24	1,01	4,08	2,21	3,12	3,11126983 7	Porosity
	MC34/3	31	12	320	20	35	120	Pull	45	70	4,37	5,73	0,68	2,01	4,09	1,74	3,1	3,09005663 4	

	MC34/4	31	12	320	20	35	120	Pull	45	75	4,87	5,14	1,69	1,37	3,78	2,38	3,45	3,44361002 4	Porosity
ref. MC18	MC35/1	31	12	320	20	35	75	Push	45	60	5,02	7,3	0,86	2,71	4,38	1,46	3,55	3,54967604 2	
	MC35/2	31	12	320	20	35	75	Push	45	65	4,71	6,78	2,23	3,17	4,21	1,94	3,34	3,33047293 9	
	MC35/3	31	12	320	20	35	75	Push	45	70	4,33	7,19	1,4	2,76	4,32	1,28	3,07	3,06177236 3	
	MC35/4	31	12	320	20	35	75	Push	45	75	3,73	6,46	1,01	2,41	4,68	1,04	2,64	2,63750829 4	
ref. MC32	MC36/1	31	12	320	20	35	60	Push	45	60	5,57	7,26	1,4	2,03	4,16	1,46	3,94	3,93858477 1	
	MC36/2	31	12	320	20	35	60	Push	45	65	5,53	6,93	1,81	2	3,72	1,37	3,92	3,9103005	
	MC36/3	31	12	320	20	35	60	Push	45	70	4,37	6,3	1,88	1,8	4,11	1,06	3,1	3,09005663 4	
	MC36/4	31	12	320	20	35	60	Push	45	75	4,66	6,56	1,43	4,03	4,26	1,32	3,3	3,2951176	
<b>PULSED – Step E</b>																			
trim factor:50																			
ref MC17	MC37	25,5	8,5	220	20	35	60	Push	45	48	4,87	6,28	2,07	2,91	3,47	1,05	3,45	3,44361002 4	
ref MC18	MC38	25,5	8,5	220	20	35	75	Push	45	48	4,83	5,9	2,78	2,06	4,04	1,16	3,42	3,41532575 3	
ref MC32	MC39	25,5	9,5	230	20	35	60	Push	45	48	5,68	6,4	3,3	4,07	2,97	1,19	4,02	4,01636651 7	
ref MC31	MC40	25,5	9,5	230	20	35	75	Push	45	48	4,87	6,3	3,19	3,52	3,63	1,07	3,45	3,44361002 4	
ref MC35/3	MC41	25,5	12	260	20	35	75	Push	45	70	3,1	6,49	0,68	3,52	4,29	1	2,2	2,19203102 2	
ref MC35/4	MC42	25,5	12	260	20	35	75	Push	45	75	3,34	5,87	0,68	2,21	4,48	1,07	2,37	2,36173664 9	
ref MC35/5	MC43	25,5	12	260	20	35	60	Push	45	60	4,27	6,7	0,89	4,38	3,79	1,31	3,02	3,01934595 6	
ref MC36/4	MC44	25,5	12	260	20	35	60	Push	45	75	3,48	5,51	2,02	6,15	4,82	1	2,47	2,46073159 9	
ref MC27	MC45	25,5	8,5	220	20	35	75	Pull	45	48	3,69	6,03	1,08	3,49	4,01	1,1	2,61	2,60922402 3	
ref MC2	MC46	25,5	8,5	220	20	35	75	Push	90	48	4,5	6,3	1,38	4,03	3,94	0,79	3,19	3,18198051 5	
ref MC22	MC47	25,5	9,5	230	20	35	60	Pull	45	48	3,58	6,17	0,48	1,12	3,89	0,81	2,54	2,53144227 7	Porosity
ref MC26	MC48	25,5	9,5	230	20	55	75	Pull	45	48	4,2	6,03	0,89	2,35	4,03	1,9	2,97	2,96984848 1	

\* Reference tests from Hammersberg & Olsson (2013)

